NUWC-NPT Technical Report 11,845
20 December 2007

Search Path Evaluation Incorporating Object Placement Structure

John G. Baylog
Thomas A. Wettergren
USW Combat Systems Department

Naval Undersea Warfare Center Division
Newport, Rhode Island

PREFACE

This report was prepared under the Office of Naval Research's MCM Data Fusion Enabling Capability Program, Search Evaluation Task, principal investigator Thomas A. Wettergren (Code 2501).

The technical reviewer for this report was Russell Costa (Code 2511).

Reviewed and Approved: 20 December 2007

Ernest Correia
Head, USW Combat Systems Department

REPORT DOCUMENTATION PAGE

Form Approved
OMB No. 0704-0188

1. AGENCY USE ONLY *(Leave blank)*	2. REPORT DATE	3. REPORT TYPE AND DATES COVERED
	20 December 2007	

4. TITLE AND SUBTITLE

Search Path Evaluation Incorporating Object Placement Structure

5. FUNDING NUMBERS

6. AUTHOR(S)

John G. Baylog
Thomas A. Wettergren

7. PERFORMING ORGANIZATION NAME(S) AND ADDRESS(ES)

Naval Undersea Warfare Center Division
1176 Howell Street
Newport, RI 02841-1708

8. PERFORMING ORGANIZATION REPORT NUMBER

TR 11,845

9. SPONSORING/MONITORING AGENCY NAME(S) AND ADDRESS(ES)

Office of Naval Research
One Liberty Center
875 North Randolph Street, Suite 1425
Arlington, VA 22203-1995

10. SPONSORING/MONITORING AGENCY REPORT NUMBER

11. SUPPLEMENTARY NOTES

12a. DISTRIBUTION/AVAILABILITY STATEMENT

Approved for public release; distribution is unlimited.

12b. DISTRIBUTION CODE

13. ABSTRACT (Maximum 200 words)

This report describes a computationally robust approach to search path performance evaluation where the objects of search interest exhibit structure in the way in which they occur within the search space. The report describes the underlying theoretical probability basis for the search evaluation computations, and provides specific details about the implementation of the numerical method. While the method is general for searchers looking for objects with structured placement, specific examples are given that are drawn from a mine hunting application. In these examples, the object structures to be examined are the laying of mines in specific mine field patterns, and the performance criterion under evaluation is search effectiveness and its relation to object clearance. Numerical issues such as the discretization of space, the detail of representation, and the scalability of computation are discussed. The application of this theoretical foundation and the numerical methods to other search paradigms is also discussed.

14. SUBJECT TERMS

Search Theory Search Evaluation Methodologies Spatial Poisson Processes
Probability Event Space Distributed Sensor Networks Mine Hunting

15. NUMBER OF PAGES
70

16. PRICE CODE

17. SECURITY CLASSIFICATION OF REPORT	18. SECURITY CLASSIFICATION OF THIS PAGE	19. SECURITY CLASSIFICATION OF ABSTRACT	20. LIMITATION OF ABSTRACT
Unclassified	Unclassified	Unclassified	SAR

TABLE OF CONTENTS

LIST OF ILLUSTRATIONS

Figure **Page**

LIST OF TABLES

Table **Page**

SEARCH PATH EVALUATION INCORPORATING OBJECT PLACEMENT STRUCTURE

1. INTRODUCTION

This report describes a robust numerical method for evaluating the search performance of operations that involve a searcher looking for objects that are possibly arranged in a spatial structure. The problem is motivated by applications in mine hunting, where individual mines are sought in the search, yet the mines are believed to often occur with a predisposition to certain patterns. The approach taken in this development builds on previous work in developing a "theory of distributed search" for distributed sensing applications (references 1 and 2). Probabilistic representations of spatial patterns for objects are combined with probabilistic representations of a moving searcher to obtain a mathematically simplified representation of cumulative search effectiveness over time. This context provides a parametric model of search performance in terms of geometrical placements and sensing parameters. When applied to a mine-hunting context, the searcher is the mine hunter and the objects are the mines. In distributed sensing contexts, such as antisubmarine warfare (ASW), the searcher is the target of interest and the objects are the distributed sensors.

The objective here is to construct a general search evaluation capability that is independent of the search path generation process and that can be used to evaluate the relative performance of alternate search path planning approaches. As such, the mathematical models developed must encapsulate the underlying critical dependencies encountered in searching for mines, and little more. Spatially dependent sensing performance, spatially dependent object likelihoods, and overlapping search patterns are all examples of the non-trivial dependencies that are critical to the mine-hunting application. By establishing these components on a mathematical probability and numerical analysis basis (as opposed to reliance on application-specific detail), it is anticipated that the dual problem of distributed sensing will be a simple extension of the search evaluation capability. The application-specific components of mine hunting are then left to a preprocess that translates them into the geometry, dynamics, and mathematical probability descriptions that are used in the evaluation capability itself.

1.1 SEARCH THEORY IN HISTORICAL APPLICATIONS

The search for objects under motion given uncertainty is a classic problem in search theory that has been well studied in the naval application domain (references 3 – 6). General search expressions for the probability of successfully completing searches in nominal environments are well known (references 3 and 4), and extensions to determine optimal search strategies in these nominal environments have also been well established (references 5 and 6). This rigorous theoretical basis is useful to understanding the basic structure of search evaluation, but becomes numerically untenable (due to many complex integrals) in all but the most trivial of environments.

The employment of search theories in analyses creates a meaningful mathematical mapping from the descriptions of sensors, targets, and searchers to the probabilistic representations of the expected outcomes of the search. By careful study of the probabilistic performance representations, operational commanders are able to more effectively allocate resources to a search, modify search plans, or create expectations on the length of time needed to achieve a search goal. The extents to which these procedures are automated are the subject of many on-going studies, and are not the topic of this report. However, for either a human or automated decision-maker to make confident search decisions requires a robust capability for assessing the search performance. When the scenario description is more complicated than the nominal considerations found in standard theory, numerical methods must be employed to effectively evaluate the search. The standard approach to dealing with the added complexity is to discretize the search space to a level of granularity where each cell becomes a mathematically nominal problem, and then numerically evaluate the combinatorial problem over the union of the discrete cells. Such approaches do not scale well when applied to the size of complex military operations and, thus, more computationally robust methods are required.

1.2 SEARCH THEORY IN DISTRIBUTED SENSOR NETWORK APPLICATIONS

The use of distributed sets of independent detectors in network formulations provides an extension to classical search problems. In ASW applications, the fields of passive sonobuoy sensors used to find moving targets are an example of such a network. In this context, the detection events on the individual sensors are defined to occur over intervals of time, and the occurrence of multiple detections over the sensor network is used to reduce the false alarm probability. The set of detections must occur in a spatio-temporal pattern that is consistent with expected target motion as the target traverses the field of sensors. While not a standard search problem, it has been shown (reference 2) that an extension of the notion of detection with respect to searcher activity provides a probabilistically meaningful description of sensor search performance. These are then combined using statistical sampling techniques for multiple sensors to accurately represent the total search effectiveness. In this search context the target is the searcher (the moving object) and the sensors are the objects of search (the fixed objects). The probability approach takes advantage of the spatial distribution of sensors as a prior on the sampling process, and the distribution of expected target characteristics provides a marginal on the performance of individual sensors over time. In an analogous manner, the mine-hunting problem is similar, with the spatial distribution of mine locations as a prior on the sampling process and the searcher characteristics given deterministically (equivalent to a delta function distribution for the marginal).

In both the ASW and mine-hunting paradigms, object detection is said to occur with probability P_D if it occurs anywhere within a predefined temporal interval or spatial region respectively. Let $X_s = \{\mathbf{x}_j\}_{j=1}^{N_S}$ be the set of positions of N_S objects (sensors) with detection radius R_d. Let $\mathbf{x}_T$ be the initial position of a moving searcher (target) randomly placed within search space $S \subseteq R^2$ and traveling at known constant velocity $\mathbf{v}_T$. Then, the searcher position at arbitrary time $t \in [t_0, t_0 + \Delta T]$ for initial time t_0 and fixed interval ΔT can be written as

$$\mathbf{x}_T(t) = \mathbf{x}_T(t_0) + (t - t_0) \cdot \mathbf{v}_T \tag{1}$$

Let X_d be the subset of X_s that falls within radius R_d of the searcher (target) trajectory established over the time interval ΔT. Then,

$$X_d = \left\{ \mathbf{x}_j \in X_s \middle| \left\| \mathbf{x}_j - \mathbf{x}_T(t) \right\| \le R_d, t \in (t_0, t_0 + \Delta t) \right\}. \tag{2}$$

Observe that

$$\begin{aligned} X_d &= \left\{ \mathbf{x}_j \in X_s \middle| \left\| \mathbf{x}_j - \left(\mathbf{x}_T(t_0) + (t - t_0) \cdot \mathbf{v}_T \right) \right\| \le R_d, t \in (t_0, t_0 + \Delta t) \right\}, \\ &= \left\{ \mathbf{x}_j \in X_s \middle| \mathbf{x}_j \in \Omega_T \right\}, \\ &= \left\{ \mathbf{x}_j \in X_s \middle| \left\| \mathbf{x}_T(t_0) - \left(\mathbf{x}_j - (t - t_0) \cdot \mathbf{v}_T \right) \right\| \le R_d, t \in (t_0, t_0 + \Delta t) \right\}, \\ &= \left\{ \mathbf{x}_j \in X_s \middle| \mathbf{x}_T(t_0) \in \Omega_j \right\}, \end{aligned} \tag{3}$$

where Ω_T and $\left\{ \Omega_j \right\}_{j=1}^{N_S}$ denote subsets of S centered about the respective searcher (target) and object (sensor) relative motion trajectories and extending in any direction to a distance of R_D. This is shown graphically in figure 1 for the case of upward searcher (target) motion. Figure 1a depicts the ensemble of these pill-shaped regions Ω_j originating at the respective object (sensor) positions and extending downward. Figure 1b depicts a searcher (target) detection region Ω_T for a single searcher originating at the initial position and extending a distance corresponding to searcher motion over the ΔT time interval.

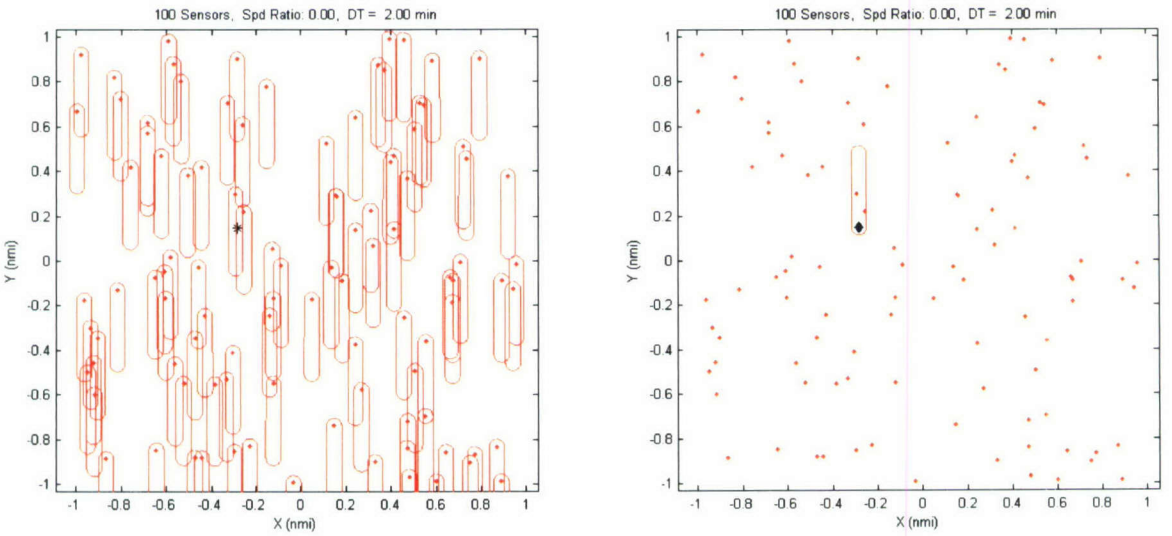

a. Target Placement Within a Sensor Pill Ensemble ***b. Object Placement Within a Target Pill***

Figure 1. Detection Event Equivalencies

In the former case, search performance is governed by computing the likelihood that a searcher (target) placement will fall within the set of sensor regions. In the latter case, the evaluation assesses the likelihood of object (sensor) placement within the searcher region. The only difference between the two cases is a frame of reference for the observer; the search performance evaluation in both cases is identical. The latter case is directly analogous to the placement of mines within a searcher region, where for mine-hunting purposes the searcher region is defined by the detection region associated with the mine-hunting platform search trajectory. The natural performance metric for either representation is the probability of successful search—that is, the cumulative probability of finding the intended object within the region covered by the searcher. The underlying probability assumption is that object placement is identically distributed (although not necessarily uniform) for each of the set of objects.

1.3 SEARCH THEORY IN MINE-HUNTING APPLICATIONS

The mine-hunting problem domain is characterized by several aspects that make it distinct from both the historical search theory and the extensions to distributed search. First, when considering the placement of stationary mines, the placement events are persistent. That is, once a mine is placed, it remains in its initial location until some form of intervention occurs to remove or disable it. Even if mines are properly identified, their presence remains in the sensor observation space unless they are removed. Secondly, sensor observations often include the detection of non-mine clutter objects (false alarms due to objects that are not the object of the search). When such objects are detected, intervention may be required to properly classify them, and the spatial density of this clutter over a search region can exhibit spatial variability.

The persistent placement event is fundamental to the search evaluation method described in this report. It is consistent with the image feature processing conducted using side-scan sonars. For any given sweep along a search path, a composite image comprising individual scans is produced—see the example shown in figure 2, which shows a typical side-scan sonar mapping of a swath of the ocean bottom and a search path conducted to find mine-like objects. The detection assessments that are performed are retained until subsequent sweeps produce additional features to process.

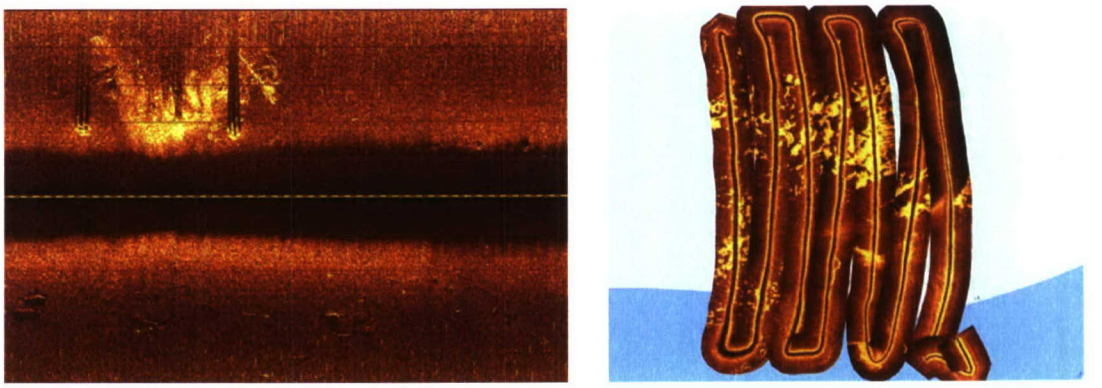

Figure 2. Example of Search Path Employing Side-Scan Sonar

The use of search theoretic methods to assess mine-hunting performance for finding random mines distributed uniformly in a region has been well established (reference 7). However, for new applications, additional factors must be considered in applying search theory to mine hunting. The actual number of mines in the search region may be unknown. There may, however, be limiting knowledge on the approximate number of mines in the region based on intelligence data, and such data must be able to be used in a probabilistic manner. The deployment of mines may not be identically distributed or even random. Mine field structure, if it exists, or any dependencies on deployment such as bathymetric constraints drive the interpretation of the expended search effort. Prior knowledge of mine field deployment patterns is especially useful when inferring mine likelihood in the region surrounding identified mines. Such patterns include barrier-like mine lines or sets of mine lines.

The effects of background clutter that can encumber the identification of mines must be taken into account. Figure 3a illustrates a spatially variable clutter density map (contours) and a numeric instantiation of mines (orange dots) and clutter (red and blue dots). Additionally, independence assumptions on detection observations using multiple sensors or multiple passes with the same search asset must be considered. The consequence of search path overlap must be integrated into the search evaluator, as complex maneuvering characteristics may exist in systems relying on fusion from multiple contacts to reduce the impact of clutter. Such a search path for high density location interrogation is illustrated in figure 3b.

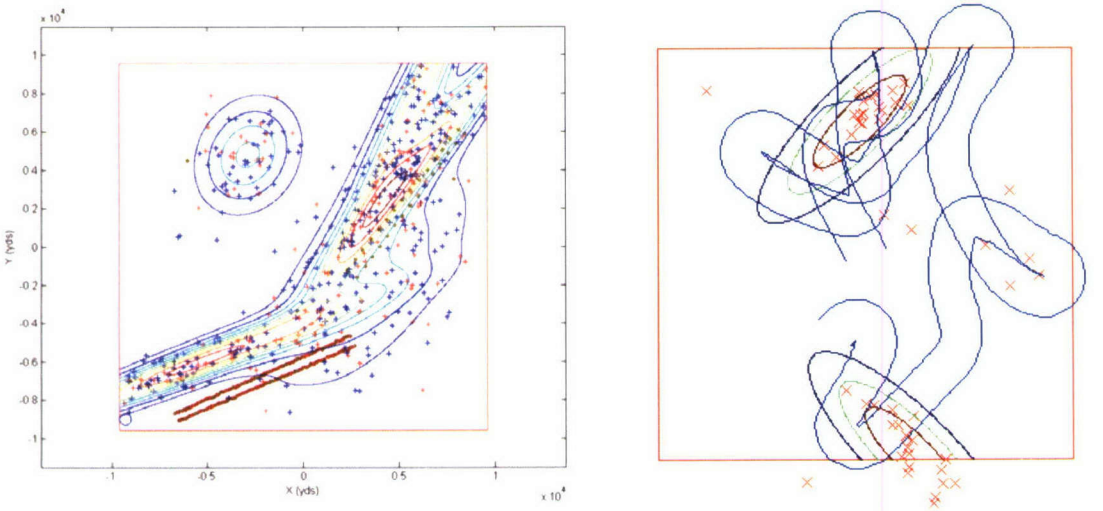

a. Clutter and Mine Field Spatial Characterization *b. Kinematic Modeling of the Search Platform*

Figure 3. Experimental Equivalencies

The objective in construction of this search path evaluation capability is to apply as much of the prior knowledge on mine field structure as is practical and relevant, while retaining flexibility in representing vehicle trajectories and sensor performance. The next section of this report describes the development of the probability event spaces over which search evaluation probabilities are calculated. This is followed by a description of the resulting search evaluation realization in a grid-based design for numerical calculation. Results are presented to articulate the performance of the evaluation capability in terms of its accuracy in probabilistic modeling and its numerical efficacy.

2. PROBABILITY EVENT SPACES FOR SEARCH PROBLEMS

This section provides the theoretical background on which the development of the search evaluation methodology is based. A review of necessary background on probability spaces and spatial Poisson processes is provided in appendix A. To facilitate the exposition, an initial simplified event context is introduced and is progressively extended to obtain the event space realizations necessary to provide an evaluation capability of sufficient utility. Necessary detail on the construction of all the event spaces is provided to illustrate how it is utilized within this tool for evaluating mine-hunting search path trajectories.

2.1 SEARCH FOR A SET OF KNOWN OBJECTS

A simple context is considered first to illustrate the event space construction. Let $S \subseteq R^2$ represent a geographic region in which to conduct a search for a set of certain objects. Assume that the set of objects is finite and that each object is known to exist within this region. Let $M = \{m_i\}_{i=1}^{N_M}$ denote the fixed set of objects placed within S, and let $\mathbf{x}_j = \langle x_j, y_j \rangle \in S$ be the location of each m_j. Furthermore, assume that these locations are unknown (hence, the need to search) and let each $\mathbf{x}_j$ be an independent random variable placed in S with probability density function $f_j(\mathbf{x}_j)$ for $\mathbf{x}_j \in S$, and zero otherwise. Then, $\langle \mathbf{x}_1, \ldots, \mathbf{x}_{N_M} \rangle$ represents an N_M-dimensional vector on S^{N_M} with probability density function

$$f(\mathbf{x}_1, \ldots, \mathbf{x}_{N_M}) = \prod_{j=1}^{N_M} f_j(\mathbf{x}_j). \tag{4}$$

The independence assumption between the placement random variables implies that each $f_j(\mathbf{x}_j)$ represents the *marginal* distribution of $\mathbf{x}_j$ on S. From this construct, the event space associated with the placement of a single object in S is considered.

Let $A \subseteq S$ be a sensor scan region within S in which one attempts to detect the objects M. The probability that an object m_j lies within A is given by

$$\Pr(\mathbf{x}_j \in A) = \int_A f_j(\mathbf{x}_j) d\mathbf{x}_j = P_A. \tag{5}$$

Since the set $\{\mathbf{x}_j \in A, \mathbf{x}_j \notin A\}$ forms a partition of S into the scan region A and its complement S\A, the probability that the object is not in A is given by

$$\Pr(\mathbf{x}_j \notin A) = \int_{S/A} f_j(\mathbf{x}_j) d\mathbf{x}_j = 1 - P_A. \tag{6}$$

This search experiment in A has two possible outcomes over a decision space $\mathcal{D} = \{d, \bar{d}\}$ corresponding to detection of the particular object or non-detection. Continuing with the assumption that object m_j lies within A, the detection event $\boldsymbol{d}_j = d$ is defined to occur with

probability $P_D = \Pr(\boldsymbol{d}_j = d \mid \mathbf{x}_j \in A)$ and the non-detection event $\boldsymbol{d}_j = \bar{d}$ to occur with probability $1 - P_D = \Pr(\boldsymbol{d}_j = \bar{d} \mid \mathbf{x}_j \in A)$. For this context, object detection is restricted to the scan region and independence between placement and detection outcomes is ascertained. The joint placement-detection outcomes $\langle \mathbf{x}_j, \boldsymbol{d}_j \rangle$ are elements of the product space $S \times \mathcal{D}$, which is partitioned as $\{\mathbf{x}_j \in A, \mathbf{x}_j \notin A\} \times \{d, \bar{d}\}$. The event space $\mathcal{F}_j = \sigma(\{\mathbf{x}_j \in A, \mathbf{x}_j \notin A\} \times \{d, \bar{d}\})$ becomes the σ–algebra generated by this partitioning. Using Bayes theorem (reference 8), the probability of detecting object m_j in A becomes

$$\Pr(\mathbf{x}_j \in A, \boldsymbol{d}_j = d) = \Pr(\boldsymbol{d}_j = d \mid \mathbf{x}_j \in A) \Pr(\mathbf{x}_j \in A) = P_D P_A . \tag{7}$$

The remaining partition probabilities are calculated in similar fashion:

$$\Pr(\mathbf{x}_j \notin A, \boldsymbol{d}_j = d) = \Pr(\boldsymbol{d}_j = d \mid \mathbf{x}_j \notin A) \Pr(\mathbf{x}_j \notin A) = 0 \cdot (1 - P_A) = 0 , \tag{8}$$

$$\Pr(\mathbf{x}_j \notin A, \boldsymbol{d}_j = \bar{d}) = \Pr(\boldsymbol{d}_j = \bar{d} \mid \mathbf{x}_j \notin A) \Pr(\mathbf{x}_j \notin A) = 1 \cdot (1 - P_A) = 1 - P_A , \tag{9}$$

$$\Pr(\mathbf{x}_j \in A, \boldsymbol{d}_j = \bar{d}) = \Pr(\boldsymbol{d}_j = \bar{d} \mid \mathbf{x}_j \in A) \Pr(\mathbf{x}_j \in A) = (1 - P_D) P_A . \tag{10}$$

Observe that non-detection of the object outside the scan region is, by definition, a certain event (as per equation (9)) and that the probabilities over all outcome partitions sum to unity. The latter occurs because a partitioning of $S \times \mathcal{D}$ produces subsets that are both mutually exclusive and collectively exhaustive.

The event space is extended by partitioning S into multiple scan regions. Following the analysis conducted in reference 7, the search space is divided into a set of identical disjoint search regions where each region constitutes an independent scan for objects. An example partitioning is illustrated in figure 4 as a set of rectangular search regions. This type of partitioning might be provided for covering a rectangular search space with a side-scan sonar. The actual shape of these disjoint regions is arbitrary as long as their union realizes the space covered by a non-overlapping search path over which the search effectiveness is to be evaluated.

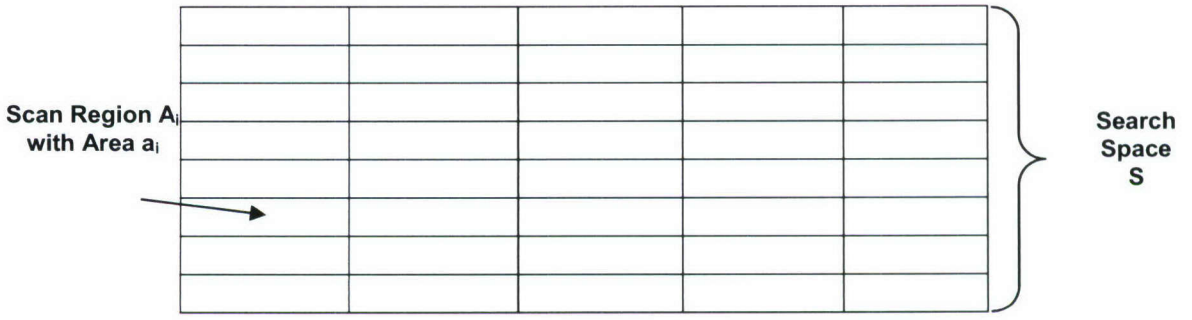

Figure 4. Search Space Partitioning

Let $\{A_i\}_{i=1}^{N_S}$ be an exhaustive partition of the search space S into a set of disjoint scan regions of equal area a_i. Throughout the sequel, the area of region A_i is represented as a_i according to

$$a_i = |A_i| = \int_{A_i} 1 \, d\mathbf{x}. \tag{11}$$

The probability that object m_j lies in region A_i, for i = 1, …, N_S, is

$$\Pr(\mathbf{x}_j \in A_i) = \int_{A_i} f_j(\mathbf{x}_j) d\mathbf{x}_j = P_{A_i}, \tag{12}$$

where it is recalled that $f_j(\mathbf{x}_j)$ is the location probability density function for object m_j. Since the partitioning is exhaustive over S, the placement of object m_j in S is certain and

$$\Pr(\mathbf{x}_j \in S) = \sum_{i=1}^{N_S} \Pr(\mathbf{x}_j \in A_i) = \sum_{i=1}^{N_S} P_{A_i} = 1. \tag{13}$$

For the moment, assume that placement and detection outcomes are independent for each scan region. Then, as above, the probability of detecting m_j in A_i becomes

$$\Pr(\mathbf{x}_j \in A_i, \boldsymbol{d}_j = d) = \Pr(\boldsymbol{d}_j = d \mid \mathbf{x}_j \in A_i) \Pr(\mathbf{x}_j \in A_i) = P_D P_{A_i}. \tag{14}$$

For notational simplicity, let E_i denote the joint event $E_i = \left\{ \left\langle \mathbf{x}_j, \boldsymbol{d}_j \right\rangle \mid \mathbf{x}_j \in A_i, \boldsymbol{d}_j = d \right\}$ representing the detection of an object that exists in region A_i. Then, $\Pr(E_i) = P_D P_{A_i}$ and the probability of not detecting object m_j in A_i becomes $\Pr(\overline{E}_i) = 1 - P_D P_{A_i}$, where $\overline{E}_i = \left\{ \left\langle \mathbf{x}_j, \boldsymbol{d}_j \right\rangle \mid \mathbf{x}_j \notin A_i \cup \boldsymbol{d}_j \neq d \right\}$ denotes the set complement with respect to the event partitions. Note that $\Pr(E_i \cap E_k) = 0, i \neq k$ as random variables are single valued in any specific realization and the scans are mutually exclusive. However, also for $i \neq k$,

$$\Pr(\overline{E}_i \cap \overline{E}_k) = \Pr(\overline{E_i \cup E_k}) = 1 - \Pr(E_i \cup E_k) = 1 - P_D(P_{A_i} + P_{A_k}). \tag{15}$$

For search path evaluation, let S_P denote a search plan comprising a subset of $\{A_i\}_{i=1}^{N_S}$. That is, $S_P = \{A_i\}_{i \in I_P}$, with I_P representing the indices corresponding to those scans conducted in a partial execution of the search plan.

Now, assume that any scanned region is searched only once. Then, the probability of detecting m_j in one of the set of disjoint scans comprising S_P becomes

$$\Pr\left(\bigcup_{i \in I_P} E_i \right) = \Pr\left(\mathbf{x}_j \in \bigcup_{i \in I_P} A_i \cap \boldsymbol{d}_j = d \right) = P_D \sum_{i \in I_P} P_{A_i}. \tag{16}$$

Observe that when S_P includes all the possible scans of the search space S, then

$$\Pr\left(\bigcup_{i=1}^{N_S} E_i\right) = \Pr\left(\mathbf{x}_j \in S \cap \boldsymbol{d}_j = d\right) = P_D \cdot 1 = P_D . \tag{17}$$

If the search is definitive in that the entire space S is searched and $P_D = 1$, then the object m_j must be found. This is shown below in the sequential update of the probability of finding object m_j in scan region k+1, given that it was not found in the previous k scans:

$$\begin{aligned}\Pr\left(E_{k+1} \mid \bigcap_{i=1}^{k} \overline{E}_i\right) &= 1 - \Pr\left(\overline{E}_{k+1} \mid \bigcap_{i=1}^{k} \overline{E}_i\right), \\ &= 1 - \frac{\Pr\left(\bigcap_{i=1}^{k+1} \overline{E}_i\right)}{\Pr\left(\bigcap_{i=1}^{k} \overline{E}_i\right)} = 1 - \frac{1 - P_D \sum_{i=1}^{k+1} P_{A_i}}{1 - P_D \sum_{i=1}^{k} P_{A_i}} = \frac{P_D P_{A_{k+1}}}{1 - P_D \sum_{i=1}^{k} P_{A_i}}.\end{aligned} \tag{18}$$

For this definitive search case, the probability of detecting object m_j in the last scan region A_{N_S}, conditioned on not finding it in any of the other regions becomes a certain event, is

$$\Pr\left(E_{N_S} \mid \bigcap_{i=1}^{N_S - 1} \overline{E}_i\right) = \frac{P_D P_{A_{N_S}}}{1 - P_D \sum_{i=1}^{N_S - 1} P_{A_i}} = \frac{1 \cdot P_{A_{N_S}}}{1 - 1 \cdot (1 - P_{A_{N_S}})} = 1 , \tag{19}$$

which is as expected.

Next, to construct a more-general event space for search evaluation, some of the constraining assumptions are relaxed. In particular, the requirements on the independence between placement and detection, the requirements on spatial invariance of the detection probability P_D, and the requirements on single-scan detection assumptions are removed. To do this, a search space partition is constructed that is a refinement of the partitioning according to scan regions. Specifically, the search space is partitioned into a uniform grid over the placement position coordinates, and probability cells are defined about the grid points. Then, as above, the probability that object m_j lies within grid cell (k,l) is given by

$$P_{G_{k,l}} = \Pr(\mathbf{x}_j \in G_{k,l}) = \int_{G_{k,l}} f_j(\mathbf{x}_j) d\mathbf{x}_j . \tag{20}$$

Since the probability density function $f(\mathbf{x}_1, \ldots, \mathbf{x}_{N_M})$ is defined to have support on S, the detection probability conditioned on placement within grid cell (k,l) becomes

$$P_{D_{k,l}} = \Pr(\boldsymbol{d}_j = d \mid \mathbf{x}_j \in G_{k,l}) = \frac{\Pr(\boldsymbol{d}_j = d, \mathbf{x}_j \in G_{k,l})}{\Pr(\mathbf{x}_j \in G_{k,l})} = \frac{\int_{G_{k,l}} \Pr(\boldsymbol{d}_j = d \mid \mathbf{x}_j) f_j(\mathbf{x}_j) d\mathbf{x}_j}{\int_{G_{k,l}} f_j(\mathbf{x}_j) d\mathbf{x}_j},$$
$$= \int_{G_{k,l}} \Pr(\boldsymbol{d}_j = d \mid \mathbf{x}_j) f_j(\mathbf{x}_j \mid \mathbf{x}_j \in G_{k,l}) d\mathbf{x}_j. \qquad (21)$$

The term $\Pr(\boldsymbol{d}_j = d \mid \mathbf{x}_j)$ represents the traditional sensor performance prediction of the probability of detection. Observe that, if sufficient resolution in the grid spacing is attained such that $f_j(\mathbf{x}_j \mid \mathbf{x}_j \in G_{k,l})$ is nearly constant over the grid cell, then

$$P_{D_{k,l}} \approx \frac{\int_{G_{k,l}} \Pr(\boldsymbol{d}_j = d \mid \mathbf{x}_j) \bar{f}_j \, d\mathbf{x}_j}{\int_{G_{k,l}} \bar{f} \, d\mathbf{x}_j} \approx \frac{\int_{G_{k,l}} \Pr(\boldsymbol{d}_j = d \mid \mathbf{x}_j) d\mathbf{x}_j}{|G_{k,l}|}, \qquad (22)$$

where $|G_{k,l}|$ is the area of grid cell $G_{k,l}$, as given by equation (11). Thus, with a fine grid resolution $P_{D_{k,l}}$ reduces to a spatial average of the detection probability over the grid cell. Conversely, if the grid resolution is coarse relative to $f_j(\mathbf{x}_j)$, then the dependency between the detection and placement probabilities is imbedded within the calculated values in the form of the weighted average of equation (21).

For $P_{D_{k,l}} < 1$, there is a probability of $1 - P_{D_{k,l}}$ that object m_j will not be detected on the first scan opportunity. It may, however, be detected on subsequent passes if the search path crosses (or overlaps) its own trajectory. Let $I_P = \{i_p\}, i_p \in \{1, \ldots, N_S\}$ denote a scan sequence that may include repeated scans. By modeling each scan's detection observation as an independent Bernoulli trial, the waiting time W (in terms of numbers of scans before detection occurs) follows a *geometric distribution* (reference 8). That is, the probability that the first detection of object m_j will occur in cell (k,l) on the nth scan becomes

$$\Pr(W = n) = P_{D_{k,l}} (1 - P_{D_{k,l}})^{n-1}. \qquad (23)$$

The succession of first occurrence probabilities develops sequentially as repeated scans are included in the search plan. Let $\boldsymbol{d}_j(n) = d$ denote the occurrence of the first detection of object m_j within scan n and $\boldsymbol{d}_j(n) = \bar{d}$ denote the occurrence of no detections of object m_j through the first n scans. With initial values

$$P_{\boldsymbol{d}_{k,l}}(1) = \Pr(\boldsymbol{d}_j(1) = d \mid k,l) = P_{D_{k,l}} \qquad (24)$$

and

$$P_{\bar{\boldsymbol{d}}_{k,l}}(1) = \Pr(\boldsymbol{d}_j(1) = \bar{d} \mid k,l) = 1 - P_{D_{k,l}}, \qquad (25)$$

the scan progression updates for n = 2 and beyond are given by

$$P_{d_{k,l}}(n) = \Pr(\boldsymbol{d}_j(n) = d \mid k,l) = P_{D_{k,l}} \cdot P_{\bar{d}_{k,l}}(n-1), \tag{26}$$

and

$$P_{\bar{d}_{k,l}}(n) = \Pr(\boldsymbol{d}_j(n) = \bar{d} \mid k,l) = (1 - P_{D_{k,l}}) \cdot P_{\bar{d}_{k,l}}(n-1). \tag{27}$$

Observe that $P_{D_{k,l}} = 1$ for definitive search detection probabilities. In that case, all subsequent first detection probabilities in the sequence go to zero, as expected.

Without loss of generality, the cell detection probabilities can be developed based solely on a geographic basis to reflect dependency on the acoustic environment. They can also be developed as functions of a predefined vehicular search path to incorporate dependencies on proximity to the sensor. In more complex cases, any combination of geometric reference and search path for one or more sensors may be applied. For situations with specified vehicular search paths, the detection probability may need to be recalculated for each subsequent detection experiment as proximity to the sensor changes—this is reflected in the form of the sequential update. For situations with a strict geographic reference, the detection probabilities need to be calculated only once.

Given the cell detection probabilities, the event probabilities defined for the scan partitioning are evaluated over the grid partition. Let I_i designate the indices of the grid cell elements contained within the scan corresponding to event E_i. This event may comprise any component of the search plan under evaluation and may possibly overlap other scans executed within the search plan. The probability of detecting object m_j within this scan is calculated by aggregating the probabilities over the grid partition refinement, as in

$$\Pr(E_i) = \sum_{(k,l) \in I_i} P_{d_{k,l}}(n(k,l)) \cdot P_{G_{k,l}}. \tag{28}$$

This calculation accommodates scan overlap at the grid cell level. That is, first detection occurs for a specific grid cell if it occurs anywhere within that grid cell. The scan sequence probability $P_{\bar{d}_{k,l}}$ is retained individually for each grid cell element (k,l).

The event space definition for the case of a known number of objects is completed by considering the detection over the finite set of N_M objects. An inference is drawn over the set of objects $M = \{m_i\}_{i=1}^{N_M}$ by constructing event spaces pertinent to the probability question under consideration. Consider the probability of detecting all N_M objects in S, which is known as a *clearance probability*. Let

$$E_{Ci} = \bigcap_{j=1}^{N_M} \left\{ \left\langle \mathbf{x}_j, \boldsymbol{d}_j \right\rangle \mid \mathbf{x}_j \in A_i, \boldsymbol{d}_j = d \right\} \tag{29}$$

represent the joint event that all objects lie within the scan region A_i and are detected. This joint event forms a partition over $S^{N_M} \times \mathcal{D}^{N_M}$ whereby each $S \times \mathcal{D}$ subspace is partitioned identically according to the search plan. Hence, unlike the previous calculations where only the subspace under consideration was partitioned, the entire outcome space must now be considered to calculate the probability that event E_{Ci} will occur; specifically,

$$\Pr(E_{Ci}) = \prod_{j=1}^{N_M} \Pr(\mathbf{x}_j \in A_i, \boldsymbol{d}_j = d) = \prod_{j=1}^{N_M} \left[\sum_{(k,l)\in I_i} P^j_{\boldsymbol{d}_{k,l}}(n(k,l)) \cdot P^j_{G_{k,l}} \right]. \tag{30}$$

In this expression and throughout the sequel, the dependency of the grid cell probability calculations on the respective $f_j(\mathbf{x}_j)$ is implied. To calculate the clearance probability, the search region probability is calculated in each subspace and combined in the product as

$$\Pr(E_C) = \prod_{j=1}^{N_M} \Pr(\mathbf{x}_j \in \bigcup_{i\in I_P} A_i \cap \boldsymbol{d}_j = d) = \prod_{j=1}^{N_M} \left[\sum_{i\in I_P} \sum_{(k,l)\in I_i} P^j_{\boldsymbol{d}_{k,l}}(n(k,l)) \cdot P^j_{G_{k,l}} \right]. \tag{31}$$

This is a consequence of the assumption of independence between object placements. When the respective $f_j(\mathbf{x}_j)$ are identically distributed,

$$\Pr(E_C) = \left[\sum_{i\in I_P} \sum_{(k,l)\in I_i} P_{\boldsymbol{d}_{k,l}}(n(k,l)) \cdot P_{G_{k,l}} \right]^{N_M}. \tag{32}$$

Next, consider the event space corresponding to the detection of one or more objects in M. Here, the same partitions formed over $S^{N_M} \times \mathcal{D}^{N_M}$ as used for the clearance probability are again used. Let

$$E_{Di} = \bigcup_{j=1}^{N_M} \left\{ \left\langle \mathbf{x}_j, \boldsymbol{d}_j \right\rangle \mid \mathbf{x}_j \in A_i, \boldsymbol{d}_j = d \right\} \tag{33}$$

represent the joint event that at least one of the N_M objects lies within scan region A_i and is detected. Since multiple object placements are defined to be mutually independent, set complements are applied over the disjoint partitions of the outcome space to get the joint probability. In particular,

$$\begin{aligned} \Pr(E_{Di}) &= 1 - \Pr(\overline{E}_{Di}) = 1 - \prod_{j=1}^{N_M} \Pr\left(\mathbf{x}_j \notin A_i \cup \boldsymbol{d}_j \neq d\right), \\ &= 1 - \prod_{j=1}^{N_M} \left(1 - \Pr(\mathbf{x}_j \in A_i, \boldsymbol{d}_j = d)\right) = 1 - \prod_{j=1}^{N_M} \left(1 - \left[\sum_{(k,l)\in I_i} P^j_{\boldsymbol{d}_{k,l}}(n(k,l)) \cdot P^j_{G_{k,l}} \right] \right). \end{aligned} \tag{34}$$

To obtain the probability of detecting at least one of the N_M objects in a partial search plan, scan probabilities are again aggregated and combined. As above, when the $f_j(\mathbf{x}_j)$ are identically distributed,

$$\Pr(E_D) = 1 - \prod_{j=1}^{N_M} \Pr\left(\mathbf{x}_j \notin \bigcup_{i \in I_P} A_i \cup \boldsymbol{d}_j \neq d \right) = 1 - \left(1 - \left[\sum_{i \in I_P} \sum_{(k,l) \in I_i} P_{\boldsymbol{d}_{k,l}}(n(k,l)) \cdot P_{G_{k,l}} \right] \right)^{N_M} \tag{35}$$

as the probability of detecting at least one of the N_M objects.

This section concludes by focusing on the case of identical placement distributions, as it illustrates an interesting property of this event space. In this case, the detection of each of the respective objects within the search path is an independent Bernoulli trial. Let p be the probability of finding an object in the search path:

$$p = \sum_{i \in I_P} \sum_{(k,l) \in I_i} P_{\boldsymbol{d}_{k,l}}(n(k,l)) \cdot P_{G_{k,l}} \, . \tag{36}$$

Then, $\Pr(E_C) = p^{N_M}$. Similarly, with $q = 1 - p$, then $\Pr(E_D) = 1 - q^{N_M}$ or, equivalently, $\Pr(\overline{E}_D) = q^{N_M}$. More generally, let N_d be the number of objects detected in the search path and $E_{N_d=m}$ be the event in which $N_d = m$ occurs. Assuming that the order of object detection is unimportant, the probability of event $E_{N_d=m}$ occurring is given by

$$\Pr(E_{N_d=m}) = \Pr(N_d = m) = \binom{N_M}{m} p^m q^{N_M - m} \, . \tag{37}$$

Thus, the assumption of identical distributions in the placement of objects leads to a binomial distribution on the number of objects detected in the search path. While this event labeling has changed to a count indicator, the event space has not changed. Hence, $\Pr(E_C) = \Pr(N_d = N_M)$ and $\Pr(E_D) = 1 - \Pr(N_d = 0)$. Note that for sufficiently large N_M, as $N_M \rightarrow \infty$ and $p << 1$ such that $\lambda_P = N_M \cdot p$ remains finite, then

$$\Pr(E_{N_d=m}) = \Pr(N_d = m) \approx \frac{(\lambda_P)^m}{m!} e^{-\lambda_P} \tag{38}$$

by the Poisson approximation to Bernoulli trials (reference 9).

It is important to note that with identical placement distributions, the calculation of search effectiveness probability is effectively reduced from an operation on the $S^{N_M} \times \boldsymbol{\mathcal{D}}^{N_M}$ outcome space to an apparent operation on $S \times \boldsymbol{\mathcal{D}}$ through a *functional composition*. That is, the repeated operation on $S \times \boldsymbol{\mathcal{D}}$ is embedded in the functional forms of equations (32) and (35). Hence, the mappings are equivalent.

2.2 SEARCH FOR OBJECTS ARRANGED IN A PATTERN

Now, consider the construction of event spaces in the search for objects placed in predefined patterns. When objects are placed in these coordinated positions, they no longer exhibit the property of mutual independence. Indeed, the more distinctive the pattern is, the more interdependent the object placements become.

Continue with the paradigm of placing the set M of N_M known objects in the search space. Now, however, the general form of the joint probability density function is expressed as a product of conditional densities, using Bayes rule:

$$f(\mathbf{x}_1,\ldots,\mathbf{x}_{N_M}) = f_1(\mathbf{x}_1)\prod_{j=2}^{N_M} f_j(\mathbf{x}_j \mid \mathbf{x}_1,\ldots,\mathbf{x}_{j-1},). \tag{39}$$

Here $f_1(\mathbf{x}_1)$ denotes an unconditional initial object placement. This form for the joint density highlights dependency on objects previously placed in the pattern. When a sequential placement depends only on the previous placement, the joint density takes the form of

$$f(\mathbf{x}_1,\ldots,\mathbf{x}_{N_M}) = f_1(\mathbf{x}_1)\prod_{j=2}^{N_M} f_j(\mathbf{x}_j \mid \mathbf{x}_{j-1},). \tag{40}$$

Such placements often occur when objects are deployed in sequence from a moving platform, such as a ship or aircraft.

In the joint probability density formulations of equations (39) and (40), the object ordering is specific and indicative of the applied deployment strategy. Alternately, placement may be structured about a common fixed reference point, as illustrated in figure 5. The reference position may constitute a general drop location in a compound experiment in which the structure is placed in the search space as a unit. For this case, there are $2N_M + 2$ degrees of freedom realized in the field and object placement—two degrees of freedom for the general drop and two for each of the N_M objects relative to the unit center. The joint object placement density is obtained through marginalization over the field placement variable:

$$\begin{aligned} f(\mathbf{x}_1,\ldots,\mathbf{x}_{N_M}) &= \int_S f(\mathbf{x}_1,\ldots,\mathbf{x}_{N_M} \mid \mathbf{x}_{ref}) f_{ref}(\mathbf{x}_{ref})\, d\mathbf{x}_{ref}, \\ &= \int_S \left[\prod_{j=1}^{N_M} f_j(\mathbf{x}_j \mid \mathbf{x}_{ref})\right] f_{ref}(\mathbf{x}_{ref})\, d\mathbf{x}_{ref}. \end{aligned} \tag{41}$$

With this modeling paradigm, object placement is conditionally independent within the structure but reference point dependent over the search space.

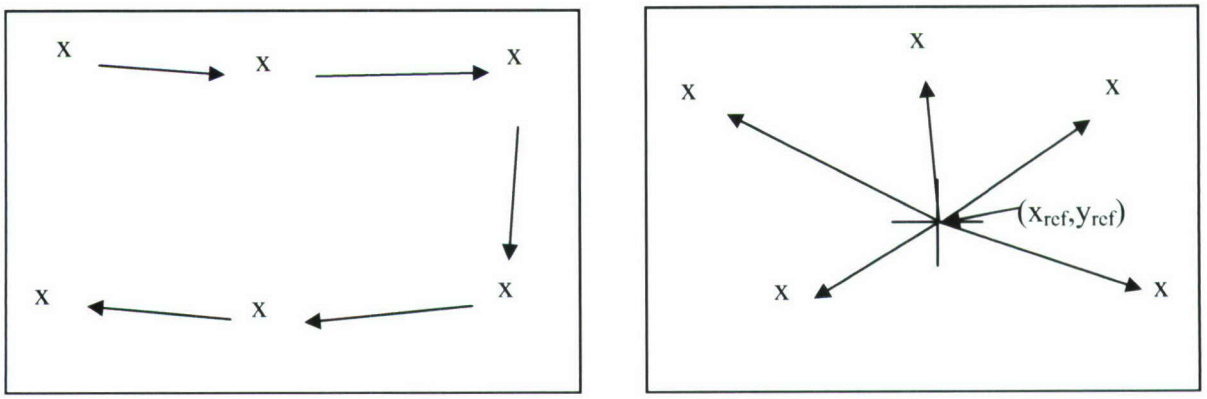

a. Sequential Placement *b. Reference Point Placement*

Figure 5. Object Placement Conditioning Variables

The properties of this object placement formulation are now examined in more detail. The patterns depicted in figure 5 are characterized by a separation between objects. Assume that object placement is restricted to occur over a set of regions $\Omega = \{\Omega_j\}_{j=1}^{N_M}$, such that

$$\mathbf{x}_j \in \Omega_j, \mathbf{x}_j \notin \Omega_i, j = 1,\ldots,N_M, i \neq j. \tag{42}$$

The set Ω constitutes the disjoint regions in R^2 over which the reference conditional probability density functions $f_j(\mathbf{x}_j \mid \mathbf{x}_{ref})$ have support; that is, $f_j(\mathbf{x}_j \mid \mathbf{x}_{ref}) = 0$ for $\mathbf{x}_j \notin \Omega_j$.

Assume that the reference location $\mathbf{x}_{ref}$ is given. Let the regions

$$R_j = \Omega_j \cap \bigcup_{i \in I_P} A_i, \tag{43}$$

for $j = 1,\ldots,N_M$, denote the intersection of the conditional support region with the partial search path. Then, the reference conditional clearance probability becomes

$$\begin{aligned} \Pr(E_C \mid \mathbf{x}_{ref}) &= \prod_{j=1}^{N_M} \Pr(\mathbf{x}_j \in \bigcup_{i \in I_P} A_i \cap \boldsymbol{d}_j = d \mid \mathbf{x}_{ref}), \\ &= \prod_{j=1}^{N_M} \int_{R_j} \Pr(\boldsymbol{d}_j = d \mid \mathbf{x}_j) f_j(\mathbf{x}_j \mid \mathbf{x}_{ref}) d\mathbf{x}_j. \end{aligned} \tag{44}$$

Here, the detection probability is considered to be independent of the reference point placement:

$$\Pr(\boldsymbol{d}_j = d \mid \mathbf{x}_j, \mathbf{x}_{ref}) = \Pr(\boldsymbol{d}_j = d \mid \mathbf{x}_j). \tag{45}$$

The clearance probability is obtained by taking the expectation of equation (44) with respect to the reference placement random variable $\mathbf{x}_{ref}$ as

$$
\begin{aligned}
\Pr(E_C) &= \int_S \Pr(E_C \,|\, \mathbf{x}_{ref}) f_{ref}(\mathbf{x}_{ref})\, d\mathbf{x}_{ref}, \\
&= \int_S \left[\prod_{j=1}^{N_M} \int_{R_j} \Pr(\boldsymbol{d}_j = d \,|\, \mathbf{x}_j) f_j(\mathbf{x}_j \,|\, \mathbf{x}_{ref})\, d\mathbf{x}_j \right] f_{ref}(\mathbf{x}_{ref})\, d\mathbf{x}_{ref}, \\
&= \int_{\bigcup_{i \in I_P} A_i} \cdots \int_{\bigcup_{i \in I_P} A_i} f(\mathbf{x}_1, \ldots, \mathbf{x}_{N_M}) \Pr(\boldsymbol{d}_{N_M} = d \,|\, \mathbf{x}_{N_M})\, d\mathbf{x}_{N_M}, \ldots, \Pr(\boldsymbol{d}_1 = d \,|\, \mathbf{x}_1)\, d\mathbf{x}_1.
\end{aligned}
\tag{46}
$$

Note that the latter form of equation (46) operates over the reference marginalized probability density function. In similar fashion, the conditional probability of detecting at least one of the objects becomes

$$
\begin{aligned}
\Pr(E_D) &= 1 - \int_S \left[\prod_{j=1}^{N_M} \left(1 - \int_{R_j} \Pr(\boldsymbol{d}_j = d \,|\, \mathbf{x}_j) f_j(\mathbf{x}_j \,|\, \mathbf{x}_{ref})\, d\mathbf{x}_j \right) \right] f_{ref}(\mathbf{x}_{ref})\, d\mathbf{x}_{ref}, \\
&= 1 - \int_S \left[1 - \sum_{j=1}^{N_M} \int_{R_j} \Pr(\boldsymbol{d}_j = d \,|\, \mathbf{x}_j) f_j(\mathbf{x}_j \,|\, \mathbf{x}_{ref})\, d\mathbf{x}_j \right. \\
&\quad + \sum_{j_1=1}^{N_M} \sum_{\substack{j_2=1 \\ j_2 \neq j_1}}^{N_M} \int_{R_{j_1}} \int_{R_{j_2}} f(\mathbf{x}_{j_1}, \mathbf{x}_{j_2} \,|\, \mathbf{x}_{ref}) \Pr(\boldsymbol{d}_{j_2} = d \,|\, \mathbf{x}_{j_2}) d\mathbf{x}_{j_2} \Pr(\boldsymbol{d}_{j_1} = d \,|\, \mathbf{x}_{j_1})\, d\mathbf{x}_{j_1} \\
&\quad \left. - \ldots \right] f_{ref}(\mathbf{x}_{ref}) d\mathbf{x}_{ref}, \\
&= \int_{\bigcup_{i \in I_P} A_i} \Pr(\boldsymbol{d}_j = d \,|\, \mathbf{x}) \left[\sum_{j=1}^{N_M} f_j(\mathbf{x}) \right] d\mathbf{x} - C,
\end{aligned}
\tag{47}
$$

where the product of reference conditional complement probabilities is expanded into a linear combination of joint probability calculations of the form used in equation (46). The parameter C denotes the remaining terms of this finite alternating series beyond the additive component. Hence, the latter form is constructed to denote an unscaled mixture minus a non-negative correction term. For a given search path, the reference conditional probability density functions $f_j(\mathbf{x}_j \,|\, \mathbf{x}_{ref})$ can change significantly with reference location. In general, the component integrals in equations (46) and (47) are distinct for each object m_j in M, and functional composition cannot be applied as in equations (32) and (35).

Consider as an example a structure comprising Gaussian components placed about the common reference point $\mathbf{x}_{ref}$. Let $\hat{\mathbf{x}}_j = \mathbf{x}_{ref} + \Delta\mathbf{x}_j$ designate the intended position of object m_j with displacement $\Delta\mathbf{x}_j$ from the reference. Assume that the structural alignment of the group of objects does not change as the reference point $\mathbf{x}_{ref}$ is moved within S. Let each object's conditional placement be distributed as $\mathbf{x}_j \sim N[\hat{\mathbf{x}}_j, \mathbf{I}_2\sigma_p^2]$ and assume that $\sigma_p << |\Omega_j|$, such that any probability mass outside Ω_j is negligible. Then, for $j = 1,\ldots,N_M$,

$$
f_j(\mathbf{x}_j \,|\, \mathbf{x}_{ref}) \approx \frac{1}{2\pi\sigma_p^2} \exp\left[-\frac{1}{2\sigma_p^2} \left((x_j - \hat{x}_j)^2 + (y_j - \hat{y}_j)^2 \right) \right], \quad \mathbf{x}_j \in \Omega_j,
\tag{48}
$$

and the joint conditional density takes the form

$$f(\mathbf{x}_1,\ldots,\mathbf{x}_{N_M}\,|\,\mathbf{x}_{ref}) = \prod_{j=1}^{N_M} f_j(\mathbf{x}_j\,|\,\mathbf{x}_{ref}),$$
$$= \frac{1}{\left[2\pi\sigma_P^2\right]^{N_M}} \exp\left[-\frac{1}{2\sigma_P^2}\sum_{j=1}^{N_M}\left((x_j-\hat{x}_j)^2+(y_j-\hat{y}_j)^2\right)\right]. \tag{49}$$

Now, let the reference placement density also be Gaussian, with $\mathbf{x}_{ref} \sim N[\hat{\mathbf{x}}_0, \mathbf{I}_2\sigma_{ref}^2]$. Following the derivation presented in appendix B, the unconditional joint density is given by

$$f(\mathbf{x}_1,\ldots,\mathbf{x}_{N_M}) = \frac{1}{\left[2\pi\sigma_P^2\right]^{N_M}}\left(\frac{\rho_p^2}{N_M+\rho_p^2}\right)\exp\left\{-\frac{1}{2\sigma_P^2}\left(\sum_{j=1}^{N_M}(x_j-\hat{x}_j)^2+(y_j-\hat{y}_j)^2\right)\right\}$$
$$\times\exp\left\{-\frac{1}{2\sigma_P^2}\left(\frac{1}{N_M+\rho_P^2}\right)\left[\left(\sum_{j=1}^{N_M}x_j-\hat{x}_j\right)^2+\left(\sum_{j=1}^{N_M}y_j-\hat{y}_j\right)^2\right]\right\}, \tag{50}$$

where $\rho_P = \sigma_P/\sigma_{ref}$ represents the ratio of individual object placement and group placement standard deviations. Note that the x and y Cartesian coordinates associated with any given object location are uncorrelated. However, the correlation between any two distinct object locations in either coordinate direction is given by the coefficient

$$\rho(\mathbf{x}_{j_1},\mathbf{x}_{j_2}) = \frac{\sigma_{j_1j_2}^2}{\sigma_{j_1}\sigma_{j_2}} = \frac{\sigma_{ref}^2}{\sigma_p^2+\sigma_{ref}^2} = \frac{1}{1+\rho_p^2}. \tag{51}$$

Such correlation highlights the loss of independence in object placement for this jointly Gaussian context.

Observe from equation (51) that when $\rho_p^2 >> 1$ the correlation between object locations is very small. This happens when field placement is very specific or when its location is inferred via the fusion of identified object locations. For this case, the independence of component placement can be assumed and

$$f_j(\mathbf{x}_j) = \frac{1}{\left[2\pi\right]\sigma_p^2\left(1+1/\rho_p^2\right)}\exp\left(-\frac{1}{2\sigma_p^2\left(1+1/\rho_p^2\right)}\left(\mathbf{x}_j-\mathbf{x}_0-\Delta\mathbf{x}_j\right)^2\right),$$
$$\approx \frac{1}{\left[2\pi\right]\sigma_p^2}\exp\left(-\frac{1}{2\sigma_p^2}\left(\mathbf{x}_j-\mathbf{x}_0-\Delta\mathbf{x}_j\right)^2\right). \tag{52}$$

However, the object locations are not identically distributed. The distinctiveness of the component densities is governed by the size of the reference point displacements relative to the drop uncertainty. Identical distribution of components can be assumed only when $|\Delta\mathbf{x}_j| << \sigma_p$.

Generally, the structure is assumed to be composed of distinct objects. Conversely, as $\rho_p^2 << 1$, the field placement uncertainty dominates and the referenced marginalized components become highly correlated but approximately identical in form. In such a case, the search problem devolves into one in which the structure itself becomes the object of the search rather than individual objects within the structure.

These two limiting conditions serve as a basis for search evaluation under a restricted type of placement. Specifically, the likelihood function for a *single object placement* is developed, where knowledge of field structure dictates the shape of the single placement density. Within this likelihood context, the capability to form accurate predictions regarding multiple detection events is lost. However, a performance assessment on the *next detection probability* can still be attained for search path comparison. To do this, the projection of the reference conditional probability density function onto a single object placement space is modeled as a mixture density. Hence, the single object placement paradigm reverts to an independent, identically distributed sampling context. Each component of the mixture density corresponds to one of the plausible object locations defined for the field structure:

$$f_m(\mathbf{x}|\mathbf{x}_{ref}) = \sum_{j=1}^{N_M} f_{m_j}(\mathbf{x}|\mathbf{x}_{ref}, m_j)\Pr(m_j). \tag{53}$$

This reference conditional density function has support over general coordinates $\mathbf{x} \in S$. The unconditional density is produced via marginalization over the field placement variable, as in equation (41), to yield

$$f_m(\mathbf{x}) = \int_S \left[\sum_{j=1}^{N_M} f_{m_j}(\mathbf{x}|\mathbf{x}_{ref}, m_j)\Pr(m_j)\right] f_{ref}(\mathbf{x}_{ref})\,d\mathbf{x}_{ref}. \tag{54}$$

In the mixture model, $\Pr(m_j)$ denotes the mixture weight corresponding to the occurrence probability for object m_j. For equation (53) to represent a proper probability density function, it is required that

$$\sum_{j=1}^{N_M} \Pr(m_j) = 1, \tag{55}$$

which is achieved through a renormalization of the individual object occurrence probabilities. The density function in equation (54) can be used to compute both the clearance probability and/or the probability of object detection in a manner analogous to equations (46) and (47), respectively.

The detection events for this construct correspond to an unstructured field placement. That is, an object can occur at any location covered by the mixture density. However, the formulation does allow for multiple instantiations occurring within the same reference field component. This is especially relevant when identical distributions are assumed in placing N_M objects in the search space. As for the unstructured placement case, when equation (35) is applied to

determine the next detection probability, the same functional composition effectively reduces the numerical computation from the $S^{N_M} \times \mathcal{D}^{N_M}$ event space to the $S \times \mathcal{D}$ subspace.

Next, the performance assessment on the next detection probability conditioned on a previously identified object is developed. The probability question now becomes finding the likely location of objects given that one of the objects has been detected and identified. Let us presume that it is unknown as to which of the ordered objects is the identified one. Let $\mathbf{x}_{id}$ denote the location of the identified object. The identified object location is related to the reference point location via

$$\mathbf{x}_{id} = \mathbf{x}_{ref} + \Delta\mathbf{x}_i + \mathbf{x}_{ei} = \hat{\mathbf{x}}_i + \mathbf{x}_{ei}, \tag{56}$$

where $\mathbf{x}_{ei} = \mathbf{x} - \hat{\mathbf{x}}_i \sim N[\mathbf{0}, \mathbf{I}_2\sigma_e^2]$ denotes a random placement error (assuming object m_i as the identified object). Assume identical error distributions $f_e(\mathbf{x})$ for each component. Then,

$$\hat{\mathbf{x}}_j = \mathbf{x}_{ref} + \Delta\mathbf{x}_j = \mathbf{x}_{id} + \Delta\mathbf{x}_j - \Delta\mathbf{x}_i - \mathbf{x}_{ei}, \tag{57}$$

and the conditional placement density function for object m_j takes the form

$$f_{m_j}(\mathbf{x} | \mathbf{x}_{id}, m_i, m_j) = \int_S f_e(\mathbf{x} - \mathbf{x}_{id} - \Delta\mathbf{x}_j + \Delta\mathbf{x}_i + \mathbf{x}_{ei}) f_e(\mathbf{x}_{ei}) d\mathbf{x}_{ei}. \tag{58}$$

These density functions (for the various m_j's) combine in a mixture form as in equation (53). Marginalizing over the field components for the identified (m_i) and anticipated (m_j) components yields the identified object placement density function:

$$f_{id}(\mathbf{x}) = \int_S \left[\sum_{i=1}^{N_M} \sum_{\substack{j=1 \\ j \neq i}}^{N_M} f_{m_j}(\mathbf{x} | \mathbf{x}_{id}, m_i, m_j) \Pr(m_j | m_i) \Pr(m_i) \right] f_e(\mathbf{x} - \mathbf{x}_{id}) d\mathbf{x}. \tag{59}$$

Generally, the mixture weights are not dependent on object location. However, if the contribution of a hypothesized component to the mixture is disallowed to enforce object separation, then the conditional mixture weights must be renormalized as

$$\Pr(m_j | m_i) = \frac{\Pr(m_j)}{1 - \Pr(m_i)}, \quad i \neq j \tag{60}$$

to guarantee a proper probability density function.

2.3 SEARCH FOR AN UNKNOWN NUMBER OF OBJECTS

When the actual number of objects for which search is conducted is unknown, the search performance evaluation must apply scrutiny over any object placement information that is given.

In the absence of any prior knowledge on the number of objects or the placement strategy, it is left to evaluate the search effort alone. Anticipatory knowledge on placement number may come in different forms, one being the expected value of the number of objects placed. To use this knowledge in developing the joint placement probability, object placement is modeled as a spatial Poisson process.

A review of spatial Poisson processes is provided in appendix A (section A.2), and an excellent overview of Poisson processes is given in reference 10. The use of Poisson processes in search theory is well studied (reference 11); they are used extensively in modeling false alarms. In summary, probability mass is assigned to every possible value of the non-negative integer n_M according to the known intensity function $\lambda(\mathbf{x})$. More specifically, for any given $A \subseteq S$, the probability of finding N(A) objects is given by

$$\Pr\left(N(A) = n_M\right) = e^{-\lambda(A)} \frac{\lambda(A)^{n_M}}{n_M!}. \tag{61}$$

When $\lambda(\mathbf{x})$ is not constant over the space S, placement occurs as a *non-homogeneous spatial Poisson process*. The coloring theorem (see appendix A, section A.2) allows us to "paint" the occurrences of objects within the space according to any independent criteria, such as detection or classification. When objects are colored according to detection and non-detection, the result is a pair of independent spatial Poisson processes.

The detection probability recursions provided in equations (26) and (27) for multiple scans of a given location can also be applied to the spatial Poisson process. At a location $\mathbf{x} \in S$, the probability of detecting an object after n previously unsuccessful search passes yields the detection coloring

$$\gamma(\mathbf{x}, n) = P_D(\mathbf{x}) \cdot P_{\overline{D}}(\mathbf{x}, n-1), \tag{62}$$

where n corresponds to the n^{th} passing of location $\mathbf{x}$ along the search path. The detection intensity function for the entire search path coverage follows as

$$\lambda_n(\mathbf{x}) = \lambda(\mathbf{x}) \sum_{j=1}^{n} \gamma(\mathbf{x}, j) = \lambda(\mathbf{x}) \cdot \gamma_n(\mathbf{x}), \quad \gamma_n(\mathbf{x}) = \sum_{j=1}^{n} \gamma(\mathbf{x}, j). \tag{63}$$

The subscript n notation is used loosely here. The intended meaning is that for any $\mathbf{x}$, $n(\mathbf{x})$ is incremented with each succeeding search pass that includes $\mathbf{x}$, and spawns yet another set of independent spatial Poisson processes over the repeated search region. Over multiple passes, the superposition theorem is applied to aggregate the intensity functions and $\lambda_n(\mathbf{x})$ denotes the aggregated intensity. For the given search path, the probability of finding objects within the grid cell $G_{k,l}$ then takes the form

$$\Pr\left(N_{k,l} = n_M\right) = e^{-\lambda_n(G_{k,l})} \frac{\left(\lambda_n(G_{k,l})\right)^{n_M}}{n_M!}. \tag{64}$$

As cells form disjoint sets in S, the independence of each $N(G_{k,l})$ allows us to develop the aggregate number of detections N_{I_P} encountered over a partial search as

$$\Pr\left(N_{I_P} = n_M\right) = e^{-\lambda_{I_P}} \frac{\left(\lambda_{I_P}\right)^{n_M}}{n_M!}, \tag{65}$$

where

$$\lambda_{I_P} = \lambda_n\left(\bigcup_{i \in I_P} A_i\right) \approx \left[\sum_{(k,l) \in \bigcup_{i \in I_P} A_i} \lambda_n(G_{k,l})\right] \approx \left[\sum_{i \in I_P} \sum_{(k,l) \in I_i} P_{d_{k,l}}(n(k,l)) \cdot \lambda_{k,l}\right], \tag{66}$$

and

$$\lambda_{k,l} = \int_{G_{k,l}} \lambda(\mathbf{x}) d\mathbf{x}. \tag{67}$$

Note that these expressions assume a grid cell resolution that is fine enough to allow assumption of constant coloring within the grid cell.

As in equation (35), equation (65) provides the basis for calculating the probability of finding at least one object along the partial search path as

$$\Pr\left(N_{I_P} \geq 1\right) = 1 - \Pr\left(N_{I_P} = 0\right) = 1 - e^{-\lambda_{I_P}}. \tag{68}$$

The Poisson process model assumes that the state variables $\mathbf{x}_j$ are identically distributed, leading to the equivalent probability representations of equations (38) and (64).

Next, the probability of detecting m objects, conditioned on a known number of objects n_M in the space S, is examined. Observe that, for a given number of objects $N(S) = n_M$ in S,

$$\Pr\left(N(S) = n_M\right) = e^{-\lambda(S)} \frac{\left(\lambda(S)\right)^{n_M}}{n_M!}. \tag{69}$$

N(S) can be decomposed into its detected and undetected components:

$$N(S) = N_d(S) + N_{\bar{d}}(S) = N_d\left(\bigcup_{i \in I_P} A_i\right) + N_{\bar{d}}(S), \tag{70}$$

where it is recognized that detections can occur only within the partial search path. Similarly, the object intensity function $\lambda(\mathbf{x})$ is decomposed into its detection and non-detection components as

$$\lambda(\mathbf{x}) = \gamma_n(\mathbf{x})\lambda(\mathbf{x}) + (1-\gamma_n(\mathbf{x}))\lambda(\mathbf{x}) = \lambda_n(\mathbf{x}) + \lambda_{\bar{n}}(\mathbf{x}),$$
$$\lambda_{\bar{n}}(\mathbf{x}) = \lambda(\mathbf{x}) - \lambda_n(\mathbf{x}). \tag{71}$$

As the detection and non-detection processes are independent, it follows that the probability of detecting m objects within the partial search path, given n_M objects in S, becomes

$$\begin{aligned}
\Pr\left(N_d\left(\bigcup_{i\in I_P} A_i\right) = m \mid N(S) = n_M \right) &= \frac{\Pr\left(N_d\left(\bigcup_{i\in I_P} A_i\right) = m \right) \Pr\left(N_{\bar{d}}(S) = n_M - m\right)}{\Pr(N(S) = n_M)}, \\
&= \left[e^{-\lambda_{I_P}} \frac{(\lambda_{I_P})^m}{m!} e^{-(\lambda(S)-\lambda_{I_P})} \frac{(\lambda(S)-\lambda_{I_P})^{n_M-m}}{(n_M-m)!} \right] \Big/ \left[e^{-\lambda(S)} \frac{(\lambda(S))^{n_M}}{n_M!} \right], \\
&= \frac{n_M!}{m!(n_M-m)!} \frac{(\lambda_{I_P})^m (\lambda_n(S)-\lambda_{I_P})^{n_M-m}}{(\lambda(S))^{n_M}}, \\
&= \binom{n_M}{m} \left(\frac{\lambda_{I_P}}{\lambda(S)}\right)^m \left(1 - \frac{\lambda_{I_P}}{\lambda(S)}\right)^{n_M-m}.
\end{aligned} \tag{72}$$

As expected, the expression in equation (72) is the same as equation (37), with the probability p represented by a ratio of intensity function evaluations. Equations (36) and (66) highlight another interesting property of the intensity function $\lambda(\mathbf{x})$. Recognizing the rate $\overline{N}$ of object placement in the space S as the integral

$$\lambda(S) = \int_S \lambda(\mathbf{x})\, d\mathbf{x} = \overline{N}, \tag{73}$$

and then normalizing $\lambda(\mathbf{x})$ by this factor yields the probability density function

$$f_m(\mathbf{x}) = \frac{\lambda(\mathbf{x})}{\int_S \lambda(\mathbf{x})\, d\mathbf{x}}. \tag{74}$$

Hence, the intensity function ratio of equation (72) takes on the form of equation (37) with

$$p = \frac{\lambda_{I_P}}{\lambda(S)} = \frac{\overline{N} \cdot \int_{\bigcup_{i\in I_P} A_i} \gamma_n(\mathbf{x}) \cdot f_m(\mathbf{x})\, d\mathbf{x}}{\overline{N}} \approx \left[\sum_{i\in I_P} \sum_{(k,l)\in I_i} P_{d_{k,l}}(n(k,l)) \cdot P_{G_{k,l}} \right]. \tag{75}$$

In general, a λ-decomposition can be performed on any intensity function to yield a probability density function for single object placement.

The application of the spatial Poisson process above enables the modeling of identically distributed object placement when the actual number of objects place is unknown. It is also

consistent with the formulation when the exact number of objects is known. The required input is in the expected rate of occurrence over the space S. As a consequence, the search evaluation procedure can model spatial variations in object placement and sensor detection performance. The model can also ingest prior knowledge of field structure when the restricted context of single object placement is applied. This can be done for the case of identified objects or for the general application of drop reference and drop preference priors.

To construct a general object density function to be applied in the evaluation of search, let us start with a random mine placement component $\lambda_R(\mathbf{x})$,

$$\lambda_R(\mathbf{x}) = \overline{N}_R \cdot f_R(\mathbf{x}), \tag{76}$$

with an expected number of randomly placed objects of $\overline{N}_R$. This intensity function presumes independent and identically distributed object placements. Let $\lambda_{ID}(\mathbf{x})$ denote the intensity function associated with a single identified object located at $\mathbf{x}_{ID}$. Then,

$$\lambda_{ID}(\mathbf{x}) = \overline{N}_{ID} \cdot f_{ID}(\mathbf{x}), \tag{77}$$

where the form of $f_{ID}(\mathbf{x})$ is that of equation (59). The parameter $\overline{N}_{ID}$ specifies the expected number of undetected objects remaining within the field structure. As noted in section 2.2, independence can be assumed if the positional uncertainty of $\mathbf{x}_{ID}$ is small relative to the field structure. That is, the next detection event could occur anywhere in which $f_{ID}(\mathbf{x})$ has support. The identical distribution assumption is valid as long as detection events are restricted to the next detection. If additional objects affiliated with this structure become identified, then $\lambda_{ID}(\mathbf{x})$ and $f_{ID}(\mathbf{x})$ would need to be updated before they can be applied again.

Consider the field prior $\lambda_{MF}(\mathbf{x})$ associated with object placement in the space S given a disposition to place objects in the designated structure. This intensity function has the similar λ-decomposition

$$\lambda_{MF}(\mathbf{x}) = \overline{N}_{MF} \cdot f_{MF}(\mathbf{x}). \tag{78}$$

For this case, the parameter $\overline{N}_{MF}$ can take on several meanings and its value must be set according to the intended assessment. Let $f_{MF}(\mathbf{x})$ take on the form of equation (54). As discussed in section 2.2, while the reference conditional density of equation (53) is conditionally independent, a large drop preference region will induce a high degree of correlation between objects that are placed first in the structure and then mapped to S. Thus, independence in placement does not hold. However, independence does hold in the placement of the structure within S. Consequently, $\overline{N}_{MF}$ can be set to indicate the expected number of field placements. The actual number of field placements may or may not be known. If known, then the density $f_{MF}(\mathbf{x})$ is applied directly in the search evaluation to assess the probability of finding the structure. If unknown, then the spatial Poisson process of equation (78) is used. Furthermore, field presence assessments can be conducted separately from next object detection probability evaluations. As every field instantiation must contain at least one object, limiting values for

$\overline{N}_{MF}$ can serve as a bound on the next detection probability. An approximate measure of performance can be achieved using the product

$$\overline{N}_{MF} = \overline{N}_F \cdot \overline{N}_{FM}, \tag{79}$$

where $\overline{N}_F$ denotes the expected number of fields and $\overline{N}_{FM}$ denotes the expected number of objects within the field. Care must be applied in deciding how to set these parameters. The size of the field structure relative to that of the drop preference density function and the size of S should be considered. Development of the methodology to set this number as a function of the field prior content is the subject of future investigations and is not discussed further.

Lastly, an aggregate intensity function can be developed as

$$\begin{aligned} \lambda(\mathbf{x}) &= \lambda_R(\mathbf{x}) + \lambda_{ID}(\mathbf{x}) + \lambda_{MF}(\mathbf{x}), \\ &= \overline{N}_R \cdot f_R(\mathbf{x}) + \overline{N}_{ID} \cdot f_{ID}(\mathbf{x}) + \overline{N}_{MF} \cdot f_{MF}(\mathbf{x}) = \overline{N} \cdot f_m(\mathbf{x}). \end{aligned} \tag{80}$$

This object intensity function summarizes general object placement conditions. Here, $\overline{N}$ denotes the total expected number of objects in S regardless of source.

2.4 ADDITIONAL CLEARANCE CONSIDERATIONS

Clearance implies the absence of undesirable objects within the space S. The probability of finding N_M known objects is given by equation (31) or equation (32), depending on the distribution of objects. While clearance implies the neutralization and/or removal of objects from the space, for the purpose of search evaluation, it is assumed that detection implies neutralization. That is, the probability of detection becomes the clearance probability as once an object is found it is incumbent on the searcher to determine how to neutralize it. More generally, other factors need to be considered for neutralization probability. Equation (46) provides the clearance probability when the field structure is known. This calculation, while specific in form, is often difficult to calculate in practice and may lose relevance when precise knowledge is unavailable. Equation (68) provides the probability of next object detection for the general case of an unknown number of objects. As the expected number of objects in S diminishes, this calculated value decreases. In the absence of new detections as the search plan is executed, a threshold can be applied to indicate a degree of clearance. Should an object become detected, the calculation must be reset and the search conducted over again.

Clearance probability can also be defined relative to the search space S. To accomplish this, the λ-decomposition of the aggregate spatial Poisson process is used and the placement conditional probability density function P_G, as defined by equation (20), is operated on. Recall from equations (25) and (27) that non-detection ($P_{\bar{d}}$) is defined globally over the space using a rectangular-grid partitioning of S. The calculated value of this probability is conditioned on object placement within the grid cell and the number of independent searches conducted over the

cell. Define $E_{\bar{d}_{k,l}}$ as the event that an object exists within cell $G_{k,l}$ and is not detected, and define $E_{\bar{d}}$ as the event that an object exists in S and is not detected. Rewriting equation (27),

$$P_{\bar{d}_{k,l}} = \Pr(E_{\bar{d}_{k,l}}) = 1 \cdot \prod_{i=1}^{N_{S_{k,l}}} \left[1 - P_{D_{k,l}}(i)\right], \tag{81}$$

where $N_{S_{k,l}}$ denotes the number of times that the cell is interrogated. The probability of event $E_{\bar{d}}$ occurring is calculated through a marginalization over S, as

$$\Pr(E_{\bar{d}}) = \sum_{(k,l)\in G} P_{\bar{d}_{k,l}} \cdot P_{G_{k,l}}. \tag{82}$$

A single object clearance criterion is then constructed as a threshold on the probability of the set complement of this event:

$$\Pr(E_d) = 1 - \sum_{(k,l)\in G} P_{\bar{d}_{k,l}} \cdot P_{G_{k,l}}. \tag{83}$$

Equation (83) provides the probability that if there is an object placed within the space S it would be detected. The density function P_G provides the basis for calculating a weighted average of the individual cell non-detection probabilities based on the spatial variability of sensor characterizations. When P_G is insufficiently defined, a diffuse prior on placement can be applied, yielding the unweighted average. As a statistic of the detection event, $\Pr(E_d)$ represents an evaluation of the search effort applied over S, rather than a measure of the likelihood of finding an object within S. Greater scrutiny on the clearance condition can be achieved by thresholding the criterion at the grid cell level in lieu of the aggregate statistic. For this case, if the threshold probability is not attained anywhere within the grid, then it is not attained over the space. This is equivalent to thresholding the probability test statistic:

$$\Pr(E_{d_{\min}}) = \min_{k,l\in G} \Pr(E_{d_{k,l}}) = 1 - \max_{k,l\in G} \left[P_{\bar{d}_{k,l}} \cdot P_{G_{k,l}} \right]. \tag{84}$$

3. SEARCH PATH EVALUATION

Drawing heavily on the development of probability event spaces presented in the preceding section, this section describes the design of a grid-based search path evaluation capability. The general requirements for this capability are fairly simple—the methods must be general enough to support evaluation of a variety of alternate search path generation techniques yet specific enough to provide realistic assessments for scenarios that exhibit a high degree of contextual complexity. For the mine-hunting application, this includes the adoption of spatially varied mine and background clutter densities and environmentally dependent sensor performance characterizations. The evaluation capability must be applicable when the number of mines in the search region is either known or unknown. In addition, the capability must support search evaluation in situations with uncertain descriptions of mine field placement structure.

3.1 GENERAL SETUP OF THE EVALUATION SPACE

Let $S \subseteq R^2$ represent a physical region in geographic coordinates and over which the search for mines is to be conducted. A grid is developed over these spatial coordinates to a resolution that accommodates the natural variability in mine placement strategies that occur due to dependencies on bathymetry, bottom composition, and geographic context (such as the proximity to harbors and shipping lanes). For simplicity of illustration, a square grid space is constructed with a rectangular *tessellation*, as illustrated in figure 6. However, the grid need not take a rectangular shape nor must the space be uniformly sampled. This simpler realization places emphasis on development of the underlying likelihood structure over which the probabilistic inferencing is conducted. Probability calculations are performed over the grid $G = \left\{ \mathbf{x} = \langle x, y \rangle \in S \mid x = \pm(k - 1/2)\Delta X,\ y = \pm(m - 1/2)\Delta Y,\ (k,m) = 1,\ldots,N_{max} \right\}$ defining the set of geographic coordinates in a square of side length $2N_{max}\Delta X$ and equal spacing $\Delta X = \Delta Y$ centered about $\langle x, y \rangle = \langle 0,0 \rangle$. Hence, $4N_{max}^2$ grid points are used to construct the space. Probabilities are updated sequentially at a time sampling that is specified to occur at regular intervals $T = \left\{ t_i \mid t_i = t_0 + i\Delta T, i = 0,1,\ldots,I_{max} \right\}$, where time t_0 indicates the start time of the search. The sampling interval ΔT is constrained to be sufficiently small relative to vehicular dynamics such that the search trajectory over this interval is approximately linear. However, the constraint of a small and uniform ΔT can be relaxed in alternate realizations without altering the likelihood structure.

In figure 6, the square search region appears on the left, with mine likelihood contours and sample objects (mines and clutter) overlaid on it. The mine locations are represented by circles and the clutter locations by plus signs. A segment of a random search path is also illustrated in the figure. The end of the search path that contains a circle and box indicates the sensor location at a current time. The box defines the region within the space used to construct a local sensor referenced map of the following form:

$$L = \left\{ \mathbf{x} \mid \mathbf{x} \in G,\ x_S - d_x \le x \le x_S + d_x,\ y_S - d_y \le y \le y_S + d_y \right\}. \tag{85}$$

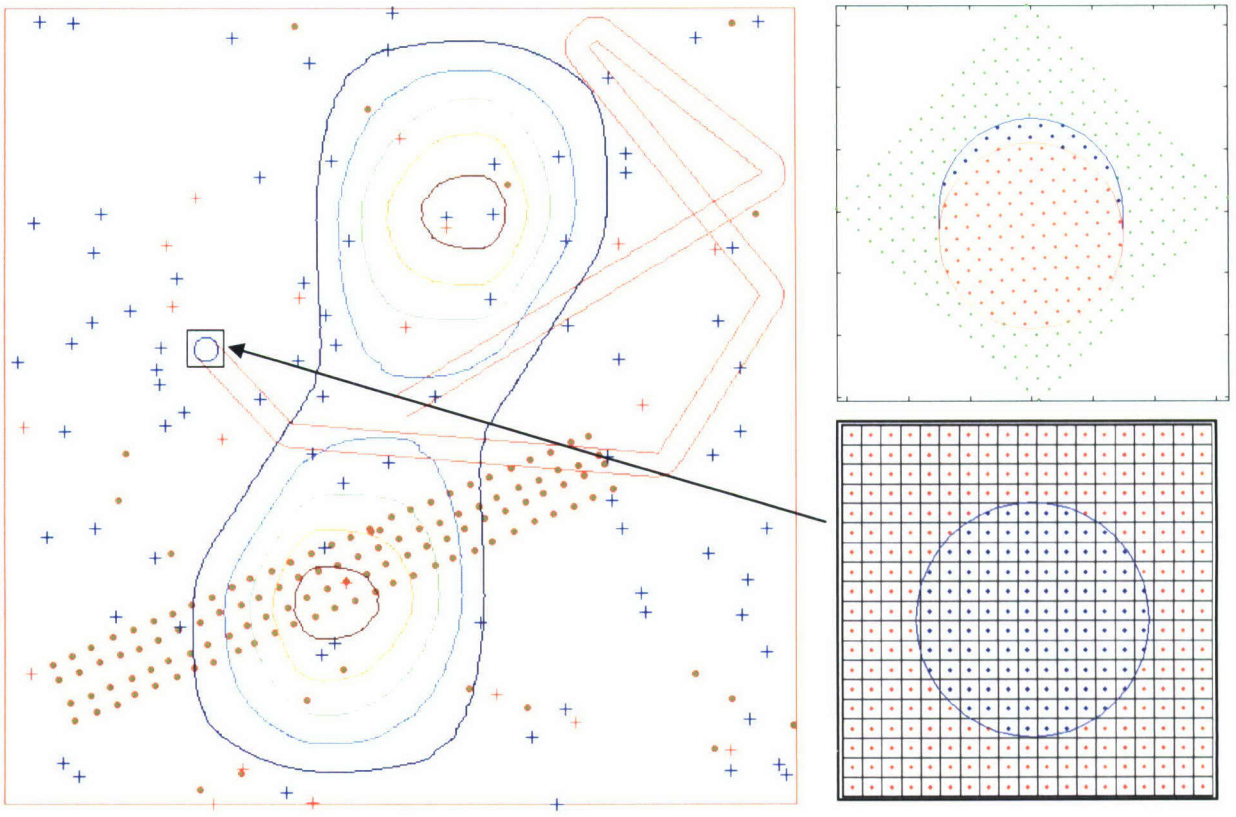

Figure 6. Evaluation Grid Development

This local map centers at the current (time = t_i) sensor coordinate reference $\mathbf{x}_S(t_i)$, as is illustrated in the lower right portion of figure 6. Here, the uniform grid spacing and the square cell construction of G becomes evident. Displacements d_x and d_y are selected to ensure that, for the given update interval ΔT, all points covered by the sensor scan along this trajectory segment are included in L. A linear transformation of coordinates in the local map at time t_i of the form

$$\mathbf{x}_{rel}(t_i) = T(\theta)\left[\mathbf{x} - \mathbf{x}_S(t_i)\right], \quad T(\theta(t_i)) = \begin{bmatrix} \cos\theta(t_i) & -\sin\theta(t_i) \\ \sin\theta(t_i) & \cos\theta(t_i) \end{bmatrix} \tag{86}$$

is applied to align coordinates with the vehicle orientation $\theta(t_i)$. This is illustrated in the upper right portion of figure 6. The circles are of radius R_D, which is indicative of the detection region covered by the sensor. Also indicated is the change of coverage as the sensor advances from time t_i to t_{i+1} along its prescribed search path. The apparent slither at the top of the circle is defined as the evaluation region.

Within the evaluation process, multiple maps are developed over these global geo-spatial coordinates, including a mine density map, a clutter density map, and a geographically referenced sensor detection map. Each of these maps associates probability mass to the grid elements, and all of the maps conform to the same grid specification G. The mine density map forms the cornerstone on which search effectiveness evaluation is conducted. As discussed in section 2.3, the mine density map is decomposed into a probability density function scaled by the expected number of mines. Globally referenced detection modeling is used to isolate geographically referenced sensor performance dependencies and to maintain the bookkeeping associated with multiple pass search paths. However, all probability calculations are made over the local sensor referenced map (over grid L).

The search region size, grid resolution, and update interval can be specified directly or can be derived as a function of three control variables—ρ_A, N_{max}, and N_{adv}. In the latter case, as above, let N_{max} specify the number of grid points in a half-length along the side of the search region. Then, setting each grid point at the center of each identical grid cell of area $\Delta x * \Delta y$, the size of search region S becomes $a_0 = |S| = 4N_{max}^2 * \Delta x * \Delta y$. Let ρ_A specify the ratio of sensor detection radius R_D to the distance advanced in a search update interval ΔT. Then, $\rho_A = R_D/D_{adv} \approx R_D/S_S\Delta T$, where $D_{adv} \approx S_S\Delta T$ for a search platform traveling at constant velocity (it is assumed that the update interval ΔT is small enough for such an approximation to hold). Let N_{adv} be a numerical resolution parameter specifying the number of grid points in the search advance slither in the direction of forward motion. Thus, the temporal update interval is given as $\Delta T = [1/\rho_A\rho_D]^+$, where $\rho_D = S_S/R_D$ and the plus brackets imply rounding up to the nearest integer value. Similarly, the grid spacing resolution in either Cartesian coordinate direction is calculated as $\Delta x = \Delta y = [D_{adv} / N_{adv}]^- = [R_D / \rho_A N_{adv}]^-$, where the minus brackets imply rounding down to the nearest integer.

This grid specification highlights interdependence between resolution and the sequential update interval determined as a function of the sensor characteristics (R_D), search rate (S_S and ΔT), and the mine field characteristics (Δx, Δy, and a_0) that are assumed. Otherwise, the size of the search region may be specified and the resulting number of grid cells necessary to attain accuracy determined. That is, either N_{max} or a_0 can be made the independent variable.

3.2 NUMERICAL CALCULATION OF SEARCH PROBABILITIES

Recall that the detection event decomposition described in section 2.1 requires that, for each grid cell, a corresponding value for the probability of detection conditioned on arbitrary mine placement within that cell be calculated as

$$P_{D_{k,l}} \approx \frac{\int_{G_{k,l}} \Pr(\boldsymbol{d} = \mathrm{d} \mid \mathbf{x}) \bar{f}\, d\mathbf{x}}{\int_{G_{k,l}} \bar{f}\, d\mathbf{x}} \approx \frac{\int_{G_{k,l}} \Pr(\boldsymbol{d} = \mathrm{d} \mid \mathbf{x})\, d\mathbf{x}}{|G_{k,l}|}, \tag{87}$$

where $|G_{k,l}|$ is the area of the grid cell, as given by equation (11). The form of equation (87) assumes constant mine placement likelihood over the grid cell, and this assumption is maintained

henceforth. As noted, the resulting detection probability represents a spatially averaged value for detection probability. When the detection likelihood within the grid cell is also approximately constant (at value P_D), equation (87) simplifies to

$$P_{D_{k,l}} \approx \frac{\int_{G_{k,l}} \Pr(\boldsymbol{d} = \mathrm{d} \mid G_{k,l})\,\mathrm{d}\mathbf{x}}{|G_{k,l}|} = \frac{P_D |G_{k,l}|}{|G_{k,l}|} = P_D\,, \tag{88}$$

as expected. Thus, under an assumption of constant detection likelihood within the grid cell, the grid cell conditional detection probability can be assimilated directly from a suitable sensor performance prediction. Note that this expression does not depend explicitly on sensor position. Rather, sensor proximity was implied in the designation of search regions and their correspondence to scans. Digressing from this restrictive association, the paragraphs below introduce the circular sensor evaluation region that is depicted in figure 6.

Let the sensor detection capability be characterized by the *definite-range law* (reference 3) with a fixed and known detection radius. That is, if the target appears anywhere within a circle of radius R_D centered at the sensor, the target will be detected by that sensor with probability P_D. Consecutive circular regions are applied for each temporal update, and the set difference as the circular region at time t_{i-1} sweeps to that at time t_i is determined. The set difference constitutes what is referred to as the evaluation region, and it is developed assuming linear motion between updates. Hence, its shape remains constant even as the search platform maneuvers about in executing its search plan. From this region, a probability change ΔP is calculated for each time interval and mapped to the event spaces under consideration.

A search path constitutes one contiguous swath centered on the vehicular trajectory established by the platform search plan. The search region is segmented along the trajectory at sampling interval $\Delta T = t_i - t_{i-1}$. This is illustrated in figure 7 for an arbitrary search path. For non-intersecting paths, the segmented search path constitutes a collection of spatial subsets that are both exclusive and exhaustive. This makes the collection well suited to set theoretic probability calculations. Note that the segments need not relate directly to specific sensor scans. All that is required is that values assigned to the geographically referenced P_D map be representative of those obtained using anticipated sensors traveling along the search trajectory. If need be, the P_D map can be developed more specifically as a function of source-receiver geometry. For this case, proximity to the search trajectory along the segment must be considered. Given a complete search path, the P_D map can be constructed over the entire geographic space prior to evaluation. However, altering the path may require that the map be updated as well.

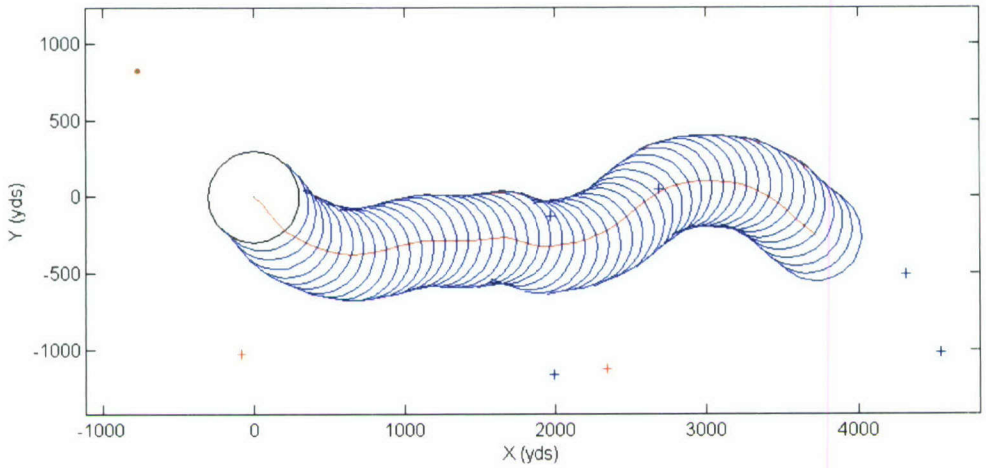

Figure 7. Example of Search Path Decomposition

For purposes of this report, the distribution of detection likelihood within the search path is of concern only for the case of intersecting search paths or when the placement density varies significantly within the search path segment. Otherwise, applying an averaged P_D to the path yields the same probability calculation. That is, if mine density is approximately constant over a region G_{Rc} comprising N_{Rc} grid cells in the set R_c as in

$$G_{Rc} = \bigcup_{(k,l)\in R_c} G_{k,l}\,, \tag{89}$$

then

$$P_{D_{Rc}} = \frac{1}{N_{Rc}} \sum_{(k,l)\in R_c} P_{D_{k,l}} = \sum_{(k,l)\in R_c} \frac{\int_{G_{k,l}} \Pr(\boldsymbol{d} = \mathrm{d} \mid G_{k,l})\,\mathrm{d}\mathbf{x}}{N_{Rc}\left|G_{k,l}\right|} = \frac{\int_{G_{Rc}} \Pr(\boldsymbol{d} = \mathrm{d} \mid G_{Rc})\,\mathrm{d}\mathbf{x}}{\left|G_{Rc}\right|}\,. \tag{90}$$

The current realization requires the development of the global P_D map to facilitate comparison of alternate search paths. However, this design requirement can be relaxed should detection probability need recalculation on a more frequent basis. For such a case, the local P_D map would be developed and applied within each update cycle in lieu of a global articulation prior to evaluation.

For the cases of intersecting search paths and/or multiple search platforms, non-detection probability must be maintained at a global scale to preserve search history. Specifically, a non-detection $P_{\overline{D}}$ map is constructed over the same grid G and initialized to unity prior to the start of the search. Then, for each time that a grid cell $G_{k,l}$ is covered by a search segment, the non-detection map is updated at the cell index k,l according to the recursion

$$P_{\overline{D}_{k,l}} = P_{\overline{D}_{k,l}}(1 - P_{D_{k,l}}) \tag{91}$$

for all the points in the evaluation region. Maintaining this quantity separately leaves the detection P_D map unchanged. The multiple pass detection probability is thus provided by the $P_D P_{\overline{D}}$ product with initial value P_D.

The probability change ΔP, over a time interval ΔT, is calculated by aggregating the joint probability for each point in the evaluation region. Let I_{i-1} represent the set of indices covered by the sensor and its evaluation region at time t_{i-1}. The set I_i is constructed to include all cell indices covered by the union of the circular sensor coverage region at time t_i and the tubular swath connecting it to the previous sensor coverage region. Then, the set difference

$$I_{\Delta i} = \left\{ (k,l) \,|\, (k,l) \in I_i, (k,l) \notin I_{i-1} \right\} \tag{92}$$

provides the indices of all grid points that lie within the evaluation region developed at time t_i. In this scheme, fringe points may occur arbitrarily within any particular update. However, the fringe points are aggregated only once per distinct search path, and so the integrity of the calculation is preserved over paths of arbitrary length to within the fringe accuracy. The probability change over the time interval follows as

$$\Delta P_i = \sum_{(k,l)\in I_{\Delta i}} P_{D_{k,l}} P_{\overline{D}_{k,l}} \cdot P_{G_{k,l}} \,. \tag{93}$$

The quantity P_G represents the probability density function provided in the prior knowledge specification or extracted from the decomposition of the mine density function when the number of mines is unknown. Hence, ΔP_i represents the probability of detecting a mine within the evaluation region conditioned on there being at least one mine within the search space S.

For the case of an unknown number of mines, the mine density function is given by $\lambda_M = \overline{N}_M \cdot P_G$, where $\overline{N}_M$ denotes the expected number of mines in the search region S. A value for $\overline{N}_M$ must be provided in the prior specification. Then, the expected number of mine detections in the evaluation region becomes $\overline{N}_{M_{Di}} = \overline{N}_M \cdot \Delta P_i$, and the probability of not finding any mines in the evaluation region becomes

$$\Delta Q_{SS_i} = \exp\left[- \overline{N}_M \cdot \Delta P_i \right] . \tag{94}$$

The aggregate non-detection and detection probabilities over the partial search path, up to and including segment i, become

$$\begin{aligned} Q_{SS_i} &= \prod_{j=0}^{i} \Delta Q_{SS_j} = \Delta Q_{SS_i} Q_{SS_{i-1}} , \\ P_{SS_i} &= 1 - Q_{SS_i} , \end{aligned} \tag{95}$$

respectively. Analogous quantities are developed for the case of the clutter density map $\lambda_C = \overline{N}_C \cdot P_{Gc}$, where the value of $\overline{N}_C$—the expected number of clutter objects in S—is also assumed to be provided in the prior knowledge specification.

For the case when N_M—the actual number of mines in S—is assumed known, and each mine is assumed to be identically distributed with density function P_G, the probability calculation takes the forms developed in section 2.1. In such a case, the clearance probability for finding all N_M mines in the partial search path is calculated as

$$P_{CP_i} = \left(\sum_{j=0}^{i} \Delta P_j \right)^{N_M} . \tag{96}$$

Similarly, the probability of finding at least one of the N_M mines along the partial search path is calculated as

$$P_{MP_i} = 1 - \left(1 - \sum_{j=0}^{i} \Delta P_j \right)^{N_M} . \tag{97}$$

3.3 EXTENSIONS FOR MINE FIELD STRUCTURE

Any prior knowledge of mine field structure is integrated into this search evaluation capability in the generation of either the underlying mine density map λ_M or its component probability density P_G. The fundamental construct is the notion of a local mine field map P_{MF}, developed over a scale commensurate with the prior knowledge of field structure. This field map can be employed in a variety of ways in calculating event probabilities. The exploitation of the field maps is the subject of ongoing investigation. The following representations apply to the restricted set of probability calculations whereby identical distribution in single mine placement can be assumed.

The mine location density function λ_M is constructed as a superposition of an unstructured mine placement density and the density function associated with each candidate mine field structure:

$$\lambda_M = \overline{N}_M \cdot P_G = \lambda_R + \sum_{j=1}^{N_{MF}} \lambda_{MF_j} , \tag{98}$$

where it is recalled that $\overline{N}_M$ denotes the expected total number of mines in the search region S. Each component of λ_M is similarly decomposed as

$$\lambda_R = \overline{N}_R \cdot P_{GR} , \quad \lambda_{MF_j} = \overline{N}_{MF_j} \cdot P_{GMF_j} , \quad j = 1, \ldots, N_{MF} , \tag{99}$$

where $\overline{N}_R$ is the expected number of randomly placed mines and $\overline{N}_{MF_i}$ is the expected number of mines placed using mine field structure i. Note that $\overline{N}_{MF_i}$ may be more or less than the number of mines necessary to totally populate the structure N_{MF_i}. This can happen when the structure population is unknown or when multiple realizations of the field can be expected. For some event criteria, the value may signify only the number of mine fields in the space S.

Substituting equations (99) into equation (98) and rearranging the terms allows the probability density P_G to be formulated as a mixture density of the form

$$P_G = W_R \cdot P_{GR} + \sum_{j=1}^{N_{MF}} W_{MF_j} \cdot P_{GMF_j}, \tag{100}$$

where mixture weights are calculated as $W_R = \overline{N}_R / \overline{N}_M$ and $W_{MF_i} = \overline{N}_{MF_i} / \overline{N}_M$. In this way, P_G incorporates prior knowledge of mine field structure at a degree proportional to its anticipated occurrence. The field structure is developed in the form of a conditional probability density function as described in section 2.2. Specifically, a *drop referenced* mine field map with a central drop reference point is constructed in local mine field coordinates. With application of the drop independence assumption, this function is convolved with a *drop preference* map developed in global coordinates to obtain the resulting mixture component P_{GMF_j}. A separate drop referenced mine field map is constructed for each candidate structure. Drop preference maps may be specific to mine field structure, depending on its composition and any constraints imposed on mine types included. The grid resolution for the drop reference and drop preference maps is identical to that of the global evaluation grid G. However, the size of the map is specific to the structure. For illustration, a construction example is provided below.

Consider an example in which the parameterization of prior knowledge on field structure consists of a single mine field type with a number of mine lines $N_L = 2$. Each line consists of a fixed number of mines with known spacing D_M between them. The spacing D_L between mine lines is assumed to be fixed and known. For this example, two random placement influences are introduced. First, a Gaussian mine drop error of the form $\mathbf{x}_e \sim N[0, \mathbf{I}_2\sigma^2]$ is applied for each mine in the structure. In this example, the drop error variance σ^2 is circularly symmetric, with $\sigma = 0.13*D_M$. The second random influence is introduced in an ancillary parameter that is independent of the space S. Define the angle θ to designate the orientation of the mine field (assuming the rotation occurs about the reference point). Let $I_\theta = [\theta_0 - \Delta\theta/2, \theta_0 + \Delta\theta/2]$ represent an angular interval $\Delta\theta$ about θ_0 from which the orientation angle θ is drawn. Nominally, all ancillary random variables must be marginalized out in the construction of the mine field map. When available, statistical parameterizations of field structure are applied directly in the marginalization process. Otherwise, maximum entropy methods (reference 12) are applied to develop plausible mine locations. These entropic priors require a minimal amount of modeling assumptions in their development. An example is illustrated in figure 8a. The functional form used in developing the entropic drop referenced map shown in figure 8a is

$$f_m(\mathbf{x}) = f_{MF}(\mathbf{x} \mid \mathbf{x}_{ref}) * f_{ref}(\mathbf{x}_{ref}), \tag{101}$$

where

$$f_{MF}(\mathbf{x} \mid \mathbf{x}_{ref}) = K_{MF} \cdot \left[\max_{j \in I_{MF}} \left\{ \exp\left(- \frac{d_\rho^2(\mathbf{x}, \hat{\mathbf{x}}_j; \mathbf{0}) + (\rho d_\theta(\mathbf{x}, \hat{\mathbf{x}}_j; \mathbf{0}))^2}{2\sigma^2} \right) \right\} \right]. \tag{102}$$

In equation (102), K_{MF} is a normalization constant to ensure that equation (101) serves as a proper probability density function. I_{MF} indicates the indices of mines within the structure and d_ρ and d_θ denote radial and angular distances of the form

$$d_\rho(\mathbf{x}_1, \mathbf{x}_2; \mathbf{x}_{ref}) = \left| \rho_2 - \rho_1 \right|, \tag{103}$$

$$d_\theta(\mathbf{x}_1, \mathbf{x}_2; \mathbf{x}_{ref}, \Delta\theta) = \max\left(\max\left(\theta_2 - \Delta\theta/2 - \theta_1, 0\right), \max\left(\theta_2 + \Delta\theta/2 - \theta_1, 0\right)\right), \tag{104}$$

where $\rho_1 = \sqrt{(x_1 - x_{ref})^2 + (y_1 - y_{ref})^2}$ and $\rho_2 = \sqrt{(x_2 - x_{ref})^2 + (y_2 - y_{ref})^2}$ denote the distances from the reference point (supplied as an ancillary parameter) to the points $\mathbf{x}_1$, $\mathbf{x}_2$, and $\theta_1 = \tan^{-1}(y_1 - y_{ref}/x_1 - x_{ref})$ and $\theta_2 = \tan^{-1}(y_2 - y_{ref}/x_2 - x_{ref})$ denote the angles between $\mathbf{x}_1$, $\mathbf{x}_2$ and the coordinate axis. The radial distance of equation (103) measures the absolute difference between the two calculated radials and the angular distance of equation (104) measures the difference between the two calculated angles relative to the size of the interval $\Delta\theta$. The latter comprises an angular interval distance. Since the drop reference map is centered about the reference point location, the reference location used in equations (103) and (104) is at the coordinate origin of the mine field map, $\mathbf{x}_{ref} = \mathbf{0}_2$.

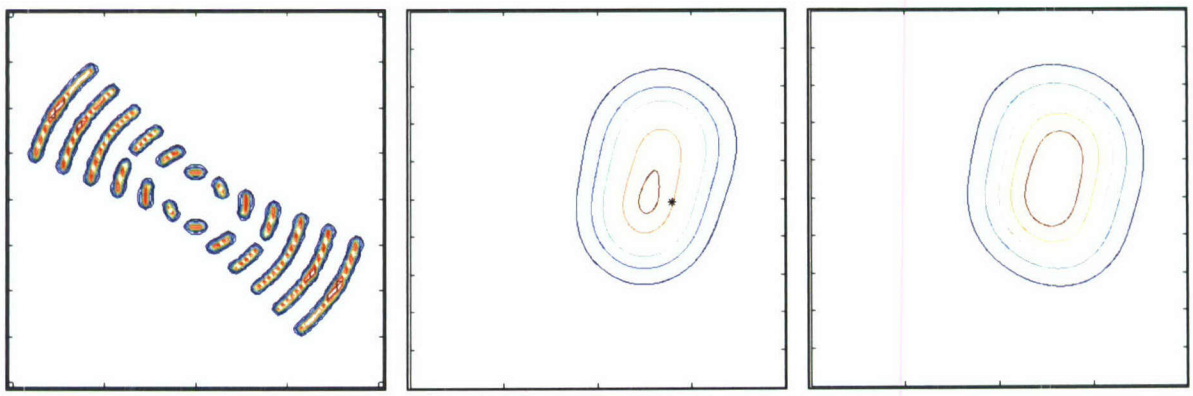

a. Drop Reference Map *b. Drop Preference Map* *c. Drop Referenced Prior*

Figure 8. Drop Referenced Prior Development

An example of a drop preference map is shown in figure 8b, and the composite drop referenced prior is generated via a numerical convolution of the drop reference and drop preference maps. The result is shown in figure 8c. Figure 9 illustrates the difference in scale between the search space and the mine field drop reference map. The size of the mine field map is indicated by the blue box in the figure. Overlaid are a replica of the drop referenced prior and a sample instantiation of a mine field consistent with the assumptions on the prior. Background clutter is depicted as the blue and red plus (+) symbols, with red indicating a mine-like appearance. The black star (*) in figure 8b represents a numerically drawn sample from the drop preference map. The sample mine field instantiation is centered at this location.

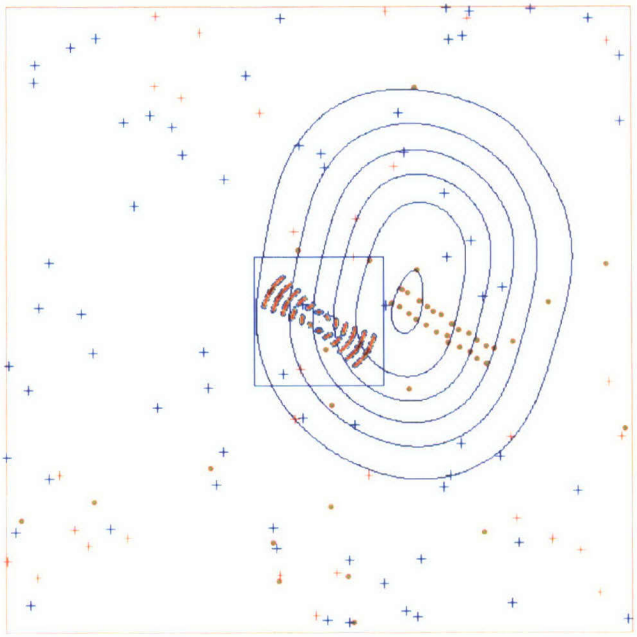

Figure 9. Example of Drop Referenced Prior

A distinct set of maps are generated when mines are known to be present in the search environment *a priori*. This is so because of the extended mixture hypotheses required to form the map as shown in equation (59). Figure 10 illustrates a sample set of the maps. The *mine location* map of figure 10a represents the uncertainty in the identified mine location. This can be merely a numerical evaluation of the drop error uncertainty or can incorporate additional factors such as registration uncertainty due to navigational errors. In the current realization, the scale of this map is set to that of the global coordinate grid G. In practice, this function has small support over S and, therefore, requires a grid that is a fraction of its current size. The global scale does accommodate multiple identified mines within the current processing methodology, provided that they do not originate from the same field structure. The *plausible location* map in figure 10b indicates where mines might be found given an identified mine location. This is a local mine field map centered on the identified mine coordinates. The current realization of this map applies only to the case of a single identified mine. Multiple mine identifications that may have originated from the same field structure require a fusion process to develop a posterior location map that is representative of the multiple observations. The map developed considers each mine

drop location represented in the mine field structure as the possible position of the identified mine. Then, for each of these points, the likelihood of other mine locations within the mine field map is evaluated and aggregated.

For purposes of illustration, the example for figure 10b utilizes an entropic parameterization in the map formation in a manner similar to the drop reference prior example, such that

$$f_m(\mathbf{x}) = f_{MF}(\mathbf{x} \mid \mathbf{x}_{ID}) * f_{ID}(\mathbf{x}_{ID}), \tag{105}$$

and

$$f_{MF}(\mathbf{x} \mid \mathbf{x}_{ID}) = K_{id} \cdot \left[\max_{\substack{j \in I_{MF}, j \neq i \\ i \in I_{MF}}} \left\{ \exp\left(- \frac{d_\rho^2(\mathbf{x}, \hat{\mathbf{x}}_j; \hat{\mathbf{x}}_i) + (\rho d_\theta(\mathbf{x}, \hat{\mathbf{x}}_j; \hat{\mathbf{x}}_i))^2}{2\sigma^2} \right) \right\} \right], \tag{106}$$

where K_{id} denotes the normalization factor. Radial and angular distance metrics are developed as in equations (103) and (104). However, the reference location $\mathbf{x}_{ref}$ now becomes the mean location for the hypothesized identified mine component; that is, $\hat{\mathbf{x}}_i$. The convolution of the mine location and plausible location maps is provided in the *field structure* prior illustrated in figure 10c.

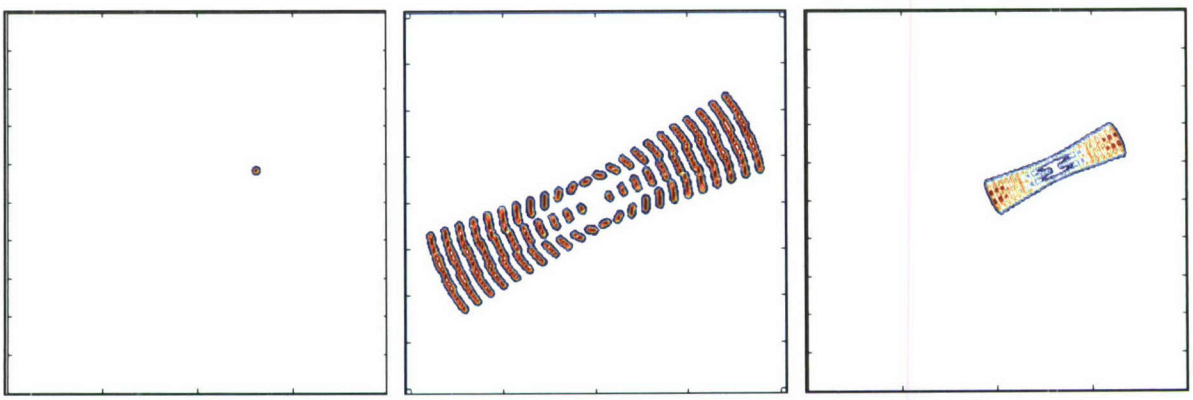

a. Mine Location Map ***b. Plausible Location Map*** ***c. Field Structure Prior***

Figure 10. Identified Mine Prior Development

The larger scale associated with the field structure prior is illustrated in figure 11. The global search space S is shown on the right and a blow-up of the field structure prior is shown on the left. The identified mine location was set to the first instantiated mine of a sample mine field drawn from the drop reference prior of the previous example. The sample mine field is discernible in the blow-up. Observe the apparent lack of likelihood at the identified mine position. This illustrates the point that the mine field structure is modeled to preclude mine

placements in close proximity to each other. It is also a consequence of the spacing included in the prior specification. Note in equation (100) that the contribution of each mine field map is weighted and aggregated. This is the case for the field structure prior as well. Hence, if the expected number of mines $\overline{N}_{MF_{ID}}$ is on the order of the other priors, the field structure prior can dominate the resulting mine density map, as occurs in figure 11. The example depicts the prior considering only one mine field type. Multiple types can be aggregated accordingly. However, the reference for any composite mine field structure remains at the identified mine location. The determination of suitable weighting between identified mines and anticipated mine field structure is part of the prior knowledge specification.

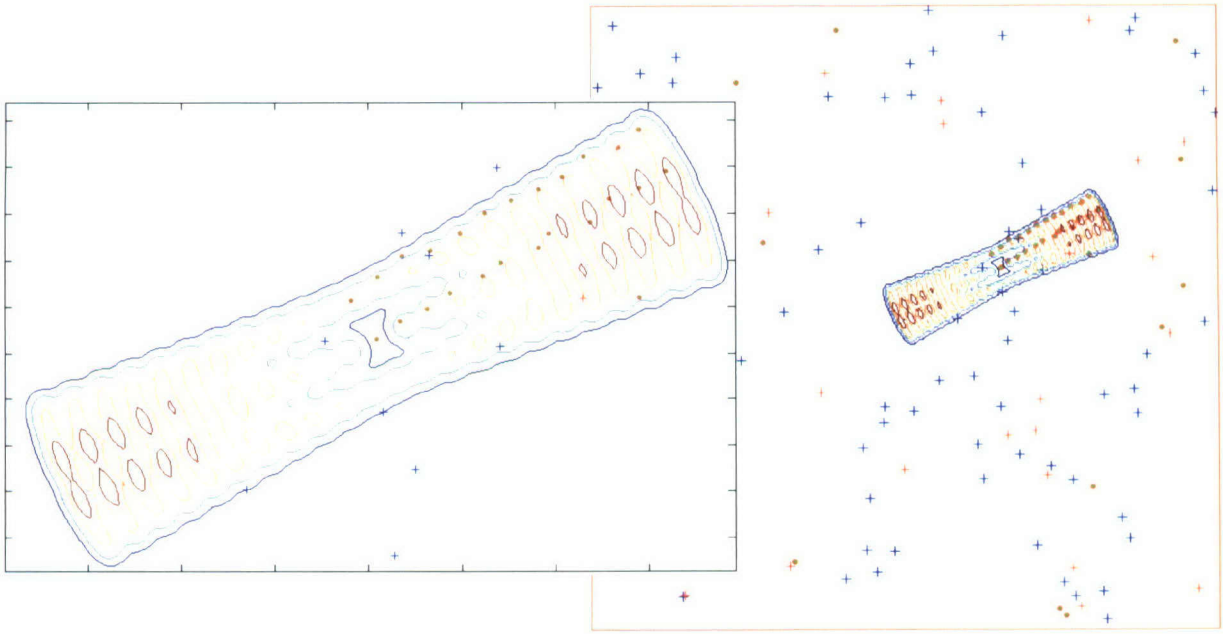

Figure 11. Example of Field Structure Prior for Identified Mines

3.4 PROCESSING DIAGRAMS

The following diagrams detail the sequence of processing steps in the computational implementation of the search evaluation capability. Figure 12 depicts the sequential evaluation loop that is realized in the algorithm. As indicated, results are provided as a function of time along the search path, and summary statistics are generated at the end of a run. The two essential processing components are the initialization block and the processing cycle conducted for each sequential update.

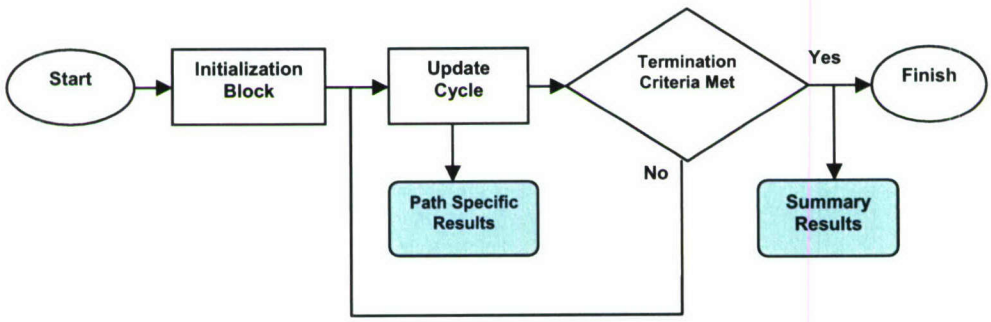

Figure 12. Sequential Evaluation Loop for Search Evaluation

In figure 13, the process initialization block is described in more detail. In particular, all prior knowledge of field structure and placement is applied in this block. The result of this prior knowledge is contained in the form of the mine and clutter density maps. The global representation of sensor performance is developed here as well. Furthermore, a search trajectory characterization process is provided within this block to synthesize search plans for basic motions. This component employs the goal-oriented curvilinear motion (GOCM) model that is described in appendix C. In practice, most search plans are provided as direct input to the evaluation program and, in such cases, this block reads that search plan into memory.

Figure 14 presents a detailed description of the update cycle itself. Here, the search path kinematic trajectory and the various evaluation maps are provided as input and operated upon. The diagram illustrates the simplicity of the modeling construct. Any processing component from which there are no outgoing flow lines indicates the availability of path-specific results. The branching of processing components illustrates opportunities for calculations to be performed in parallel. Following completion of the evaluation, summary results are produced by either extracting the path-specific results at the terminating conditions, or by operating on them in some ancillary fashion.

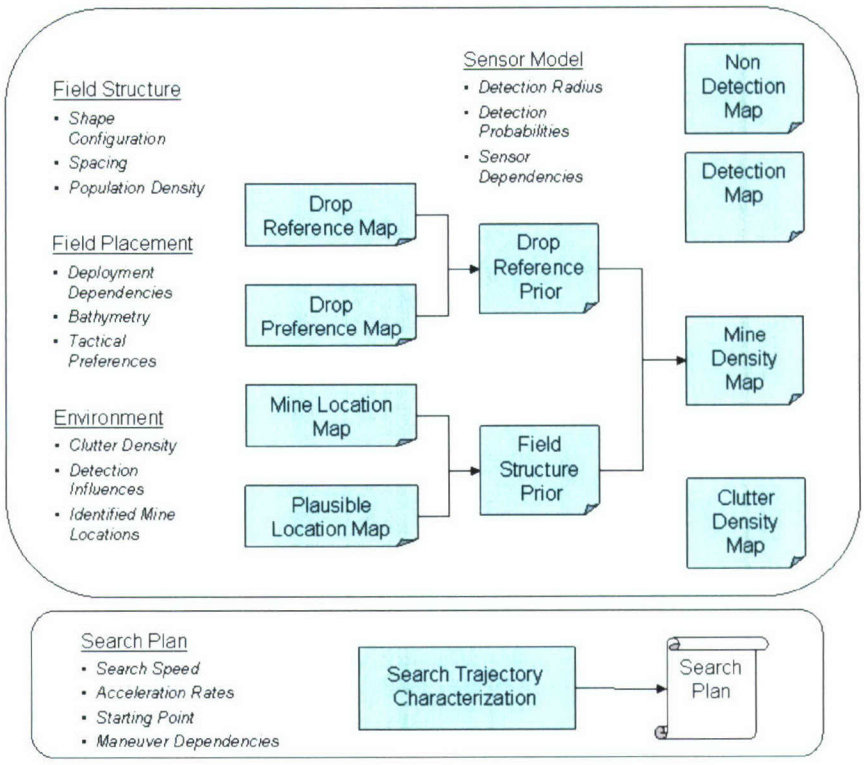

Figure 13. Initialization Block Diagram

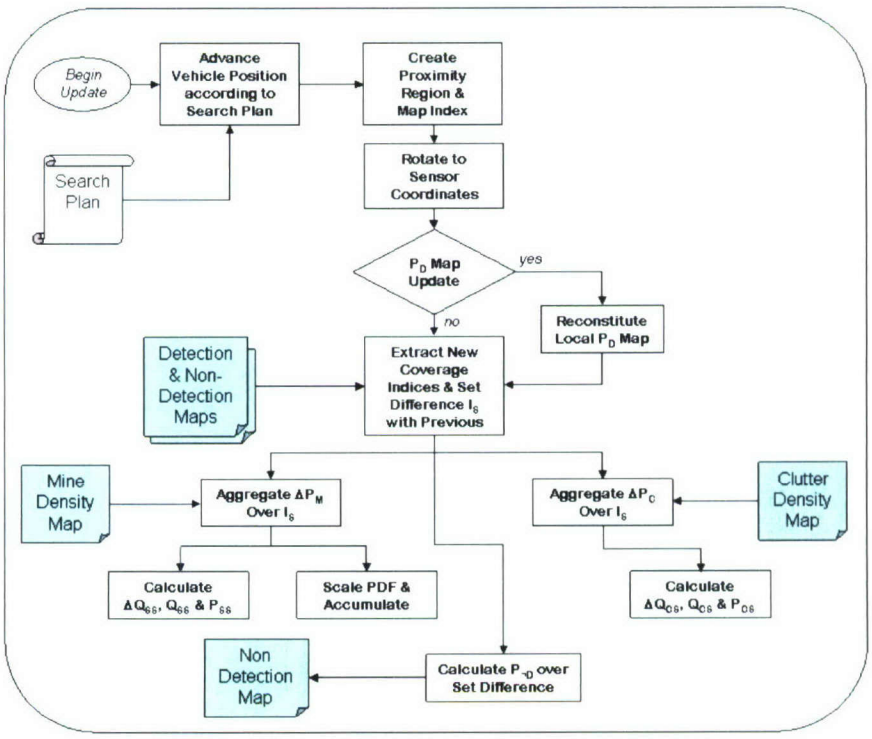

Figure 14. Update Cycle Diagram

4. ALGORITHM PERFORMANCE

This section presents results that serve to validate the search evaluation methods described in this report in terms of accuracy and utility. To the degree practical, the numerical results of the evaluation method are compared against theoretical and experimental results. The intent is to demonstrate the achieved performance for alternate grid resolutions under conditions of varying complexity.

4.1 COMPARISON AGAINST A BASELINE P_{SS}

The first level of validation under consideration is a comparison of calculated values for the probability of successful search P_{SS} against theoretical values. To do this, a "mow the lawn" type of search pattern is used where the search trajectory is set to lie entirely within the search region. In this example the search speed of the platform is set constant and the turn rate $\dot{C} = S/R_D$ is constrained to achieve constant area coverage per unit time, as discussed in appendix C. For the condition of uniformly random mine placements over the search space S, this affords a direct comparison of the search path results against an equivalent long, single-leg search path. The predicted P_{SS} yields (as a function of time) the probability of finding the next occurrence of a mine within the executed portion of the search path. It has the functional form of the Koopman's random search law (reference 3)

$$P_{SS}(t) = 1 - \exp\left[-N_M P_D \phi(t)\right], \tag{107}$$

where $N_M P_D$ represents the expected number of detected mines in the search space and

$$\phi(t) = \frac{\pi R_D^2 + 2R_D S(t - t_0)}{a_0} \tag{108}$$

defines the area swept out by the searcher over time t relative to the size of the search space. As the actual number of mines is unknown, $N_M P_D \phi(t)$ yields (as a function of time) the expected number of mines detected in the executed portion of the search path.

Figure 15 shows the sample search region used for the validation. A search speed of 10 knots is used with a search time of 8 hours and 14 minutes. Other scenario parameters include an update rate of 9 seconds, a sensor detection radius $R_D = 300$, and $P_D = 0.95$, yielding an advance ratio of $\rho_A = 6$. Using a value of $N_M = 2$, a square search region of 10,000 yards per side is selected to produce a search plan that is not dominated by straight search legs. For this experiment, a fixed resolution is used in lieu of the aforementioned scaling parameterization. Four separate numerical evaluations were run, using spatial grid resolutions of $\Delta x = \{100, 50, 25, 12.5\}$, with $\Delta y = \Delta x$ for each evaluation. The consequence on grid cell density within the sensor detection region and within the evaluation region is illustrated in figure 16. The total number of grid points required, that is $N_{tot} = (2N_{max})^2$, is affected accordingly for each case.

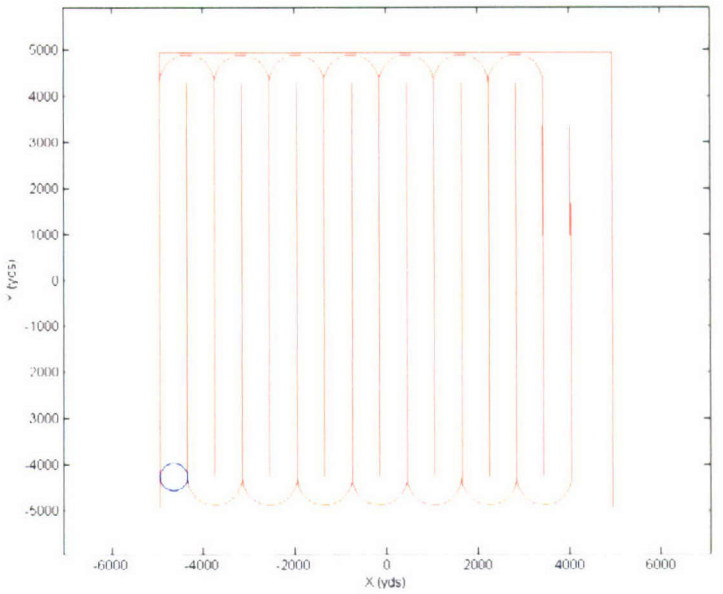

Figure 15. Search Path for Baseline P_{SS} Experiment

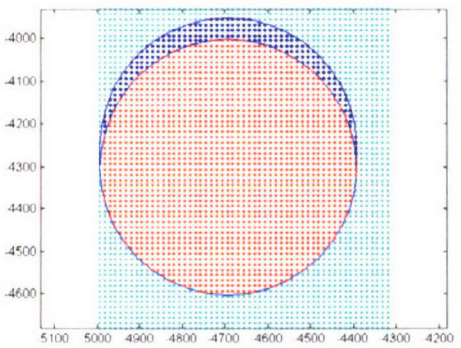

a. $N_{max} = 400$, $\Delta x = 12.5$

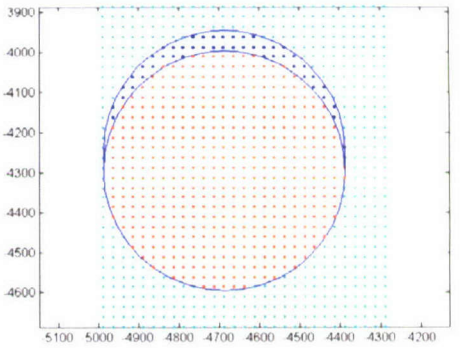

b. $N_{max} = 300$, $\Delta x = 25$

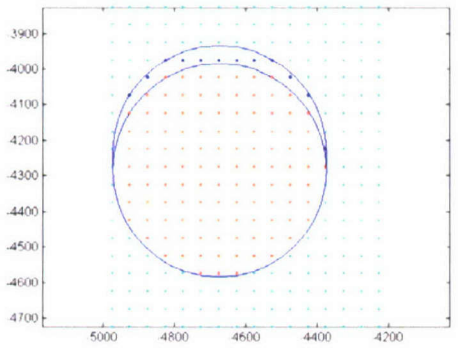

c. $N_{max} = 200$, $\Delta x = 50$

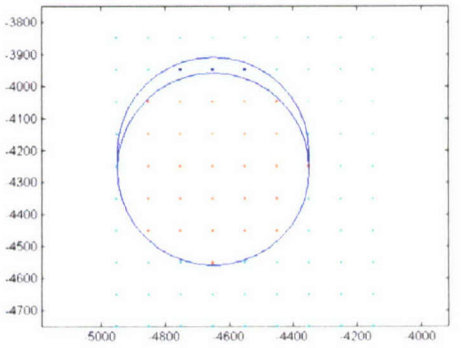

d. $N_{max} = 100$, $\Delta x = 100$

Figure 16. Example of Grid Spacing Variation

The resulting values for probability of successful search P_{SS} from the computational experiment are shown in figure 17. All four grid resolutions are depicted, although similarity of results makes it difficult to discern them in the figure. The red dots denote the calculated values of P_{SS} and are presented at a sampling of every 50 time updates. They are superimposed over the blue line depicting the theoretical value of P_{SS} using equation (107). The curve realizes Koopman's random search law as described in section 2.3 for the case where the expected number of mines in the search space, $E\{N_M\} = 2$, is known. The black and blue dots correspond to the case where the actual number of mines, $N_M = 2$, is known. The black correspond to the probability of finding both mines, while the blue correspond to finding either of them.

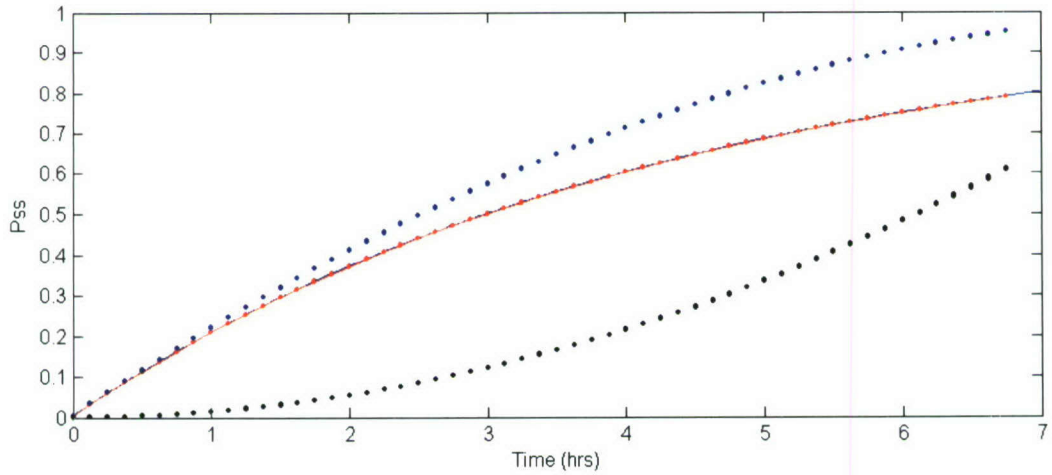

Figure 17. Probability Calculation Results

Figure 18 shows the difference error between the P_{SS} calculation and the theoretical values. All the error curves show the effect of the non-linear mapping from area coverage to probability. The impact of the platform turns in executing the search plan is least discernible (i.e., has lowest error) at the highest resolution (case A) and becomes more pronounced as resolution degrades. At the lower resolutions, the impact of grid cell alignment relative to the search plan is evident as another source of error. In the lowest resolution (case D) where the update evaluation region is smaller than the grid point separation, there is "jumpiness" in the prediction. Such sizing conditions do not present a theoretical shortfall, however, as the probability calculations are essentially set functions and it is the accuracy of the aggregated evaluation regions that drive the prediction accuracy. Each of these phenomena should be anticipated in selecting grid size and scale during a search path evaluation.

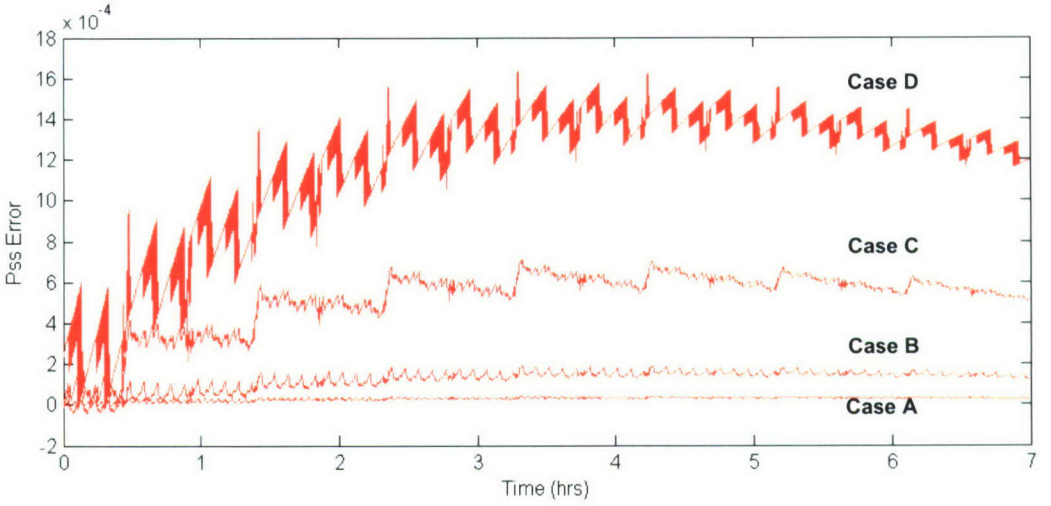

Figure 18. P_{SS} Error Over the Search Path

The numerical accuracy of the four cases is summarized in table 1. Here, the "Maximum Error" refers to the maximum difference error evaluated for P_{SS} over the search path for the given grid resolution. The "Coverage Bound" is an approximate bound reflecting a worst-case condition that is provided for comparison. This bound is based on the unusual properties of this test case. Specifically, with turn rate $\dot{C} = S/R_D$ and an aggregated turn angle of zero, the search trajectory path length is identical to that of the two coverage bounds on either side of the trajectory and that of an equivalent straight-line path had no turns been made. To show this, observe that the trajectory path length over the turn segment is

$$L_T = \theta \cdot R_D = \dot{C}\Delta T_C \cdot R_D = S\Delta T_C . \tag{109}$$

As the outer coverage boundary realizes an arc of radius $2R_D$, the outer boundary path length during the turn is twice that of the search platform trajectory, while the inner path length is zero. Hence, over a sequence of turn and counterturn, all path lengths become equal. As the grid realizes cell boundaries that consist of parallel lines in the x and y direction, for any linear segment of the search path the maximum number of grid cell interactions for a search boundary line is limited by $N_G = S\Delta T/R_D$. For curvilinear motion where the grid resolution is much smaller than the radius of curvature of the turn, the crossing of the boundary path across individual grid cells is approximately linear and N_G applies as an approximate limiting condition. Additionally, for each grid cell interaction at the boundary, the maximum error in the coverage calculation due to lateral grid overlap is on the order of one-half of the cell density value, with equivalent sized errors distributed equally on either side of the path boundary. Hence, the approximate bound $|\phi_e(t)| \le N_G \Delta x^2 / a_0$ becomes a limiting condition on the aggregated set size error. The mapping to the P_{SS} error as used in the Coverage Bound is thus

$$
\begin{aligned}
\left|P_{SSe}(t)\right| &= \left|1-\exp\left(-N_M P_D \phi(t)\right)-\left[1-\exp\left(-N_M P_D(\phi(t)+\phi_e(t))\right)\right]\right|, \\
&= \left|\exp\left(-N_M P_D \phi(t)\right)\left[\exp\left(-N_M P_D \phi_e(t)\right)-1\right]\right|, \\
&\le \exp\left(N_M P_D \left|\phi_e(t)\right|\right)-1.
\end{aligned}
\tag{110}
$$

In table 1, the error bound is significantly larger than each of the observed maximum errors. The bound is meant to serve as a worst-case indicator representative of the situation where the search trajectory lines up in the worst possible arrangement relative to the underlying grid. More typically, averaging effects lead to calculation errors accumulated over the search trajectory that are much smaller.

Table 1. P_{SS} Baseline Comparison Results

	Case A	**Case B**	**Case C**	**Case D**
Multiplier	1	2	3	4
Δx / Grid Size	12.5 / 640000	25 / 160000	50 / 40000	100 / 10000
Maximum Error	0.000043	0.000193	0.000712	0.001638
Coverage Bound	0.017703	0.035406	0.070812	0.141623

4.2 VALIDATION VIA SIMULATION EXPERIMENTS

This section presents a limited set of simulation results to authenticate the probability predictions established for the various search events described in the preceding sections. Validation is achieved over a Monte Carlo ensemble of repeated trials when the observed frequency of occurrence approaches the predicted probability as the number of samples in the experiment becomes large. These experiments are intended to be informative as well, and they serve to demonstrate how search event probabilities must be interpreted in applying the various criteria.

For all the simulation experiments, a grid specification of $\{N_{max} = 400, N_{adv} = 3, \rho_A = 4\}$ is applied, yielding a search box of 20000 yards per side and a grid of 640 thousand cells, with a resolution of 25 yards. The first experiment involves a simple "mow the lawn" search plan as above, except that the search platform broaches the search region boundary before turning to the next leg. This enables a comprehensive search of the region, as illustrated in figure 19. A uniform mine density function with the expected number of mines in the search region of $N_M = 4$ is applied, with a constant detection probability of $P_D = 0.8$ and a detection radius of $R_D = 300$ yards. The numerically computed probability assessments are shown in figure 20 for a search path extending to three sweeps of the area.

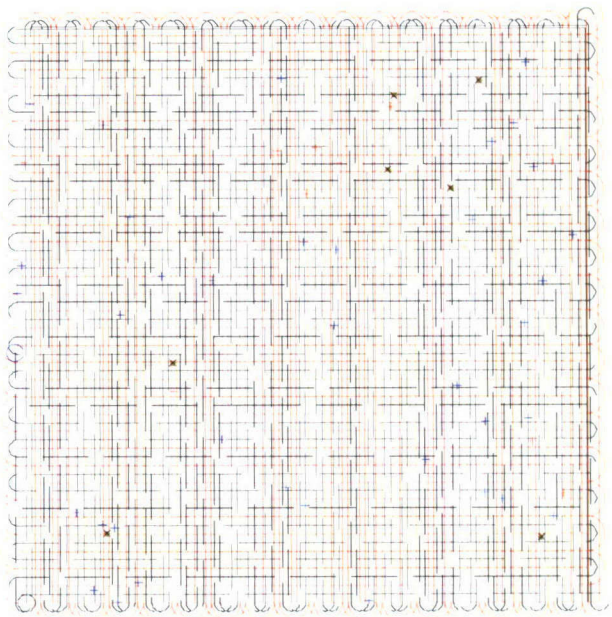

Figure 19. Search Path for the Uniform Drop Experiment

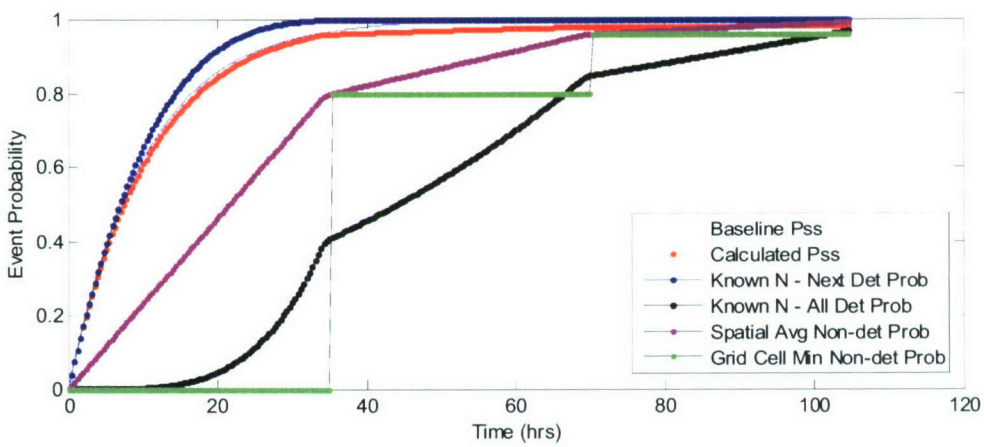

Figure 20. Search Probabilities for the Uniform Drop Experiment

First, observe in figure 20 that as coverage is applied outside the designated search area where placement likelihood is zero, search effectiveness is delayed and the calculated P_{SS} lies below the theoretical value conditioned on continuous coverage. Observe also that the next detection probability for the case of a known number of mines in the search region lies above the P_{SS} curve. This precise knowledge of the tactical situation reduces uncertainty and that is reflected in the prediction. The remaining three curves relate to area clearance probability. Observe that the spatial average clearance probability lies consistently above the probability of the known number of mines being detected. Similarly, the minimum cell clearance probability is also shown.

The first Monte Carlo experiment focuses on next detection probability and its dependency on prior knowledge of the number of mines N_M. A uniform distribution over S is applied. For the known number of mines condition, precisely four mines are placed in each experimental realization. For the unknown number case, an expected value of four mines is used and a Poisson distributed number is drawn to determine the actual number of mines to place at random for each realization. Mine locations are tagged to grid cells and, if a mine is encountered during the sequential search evaluation, a uniform random number is drawn and tested against a threshold of detection probability P_D to determine if detection occurs. The number of mines detected over the search path is recorded and a test statistic is set to 1 if a detection occurred and to 0 otherwise. A partial search path is examined for this experiment with results generated when the predicted P_{SS} attains a value of 0.8. This yields a first detection probability of 0.8725 for the case of known N_M and provides a context where the predictions are distinct. Figure 21 presents the ensemble average of this test statistic as a function of the number of ensemble realizations (note that the horizontal axis of figure 21 is logarithmic). Observe that as the number of realizations approaches 1000, the observed frequencies of occurrence converge to their predicted values, such that a separation between outcomes is readily apparent.

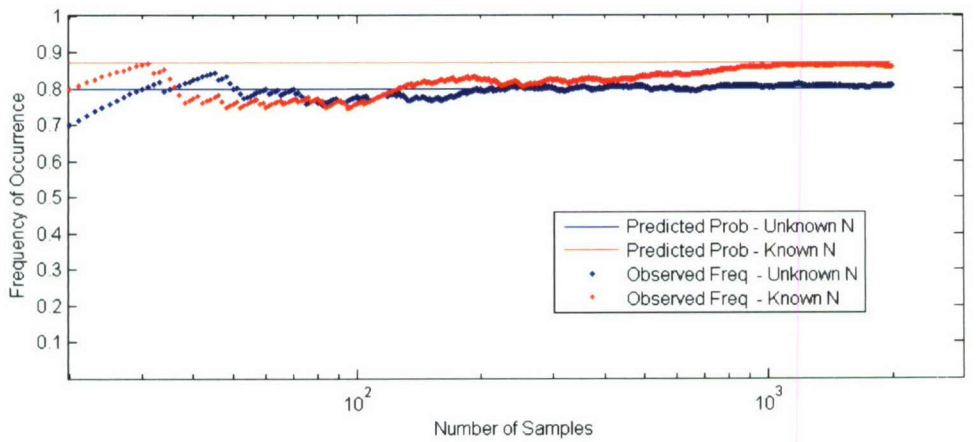

Figure 21. Partial Search Path Mine Detection Results

Next, consider a clearance search path comprising an entire sweep of the search region. For this Monte Carlo experiment, two clearance events are considered. Given precise knowledge of the number of mines N_M, the predicted probability of detecting all of them is compared to the

observed frequency of occurrence. To do this, the number of mines that are detected over the search path is recorded. The test statistic is set to 1 if this number equals the known value and to 0 otherwise. Results are plotted in figure 22. The other clearance event involves the search effort assessment given no knowledge of mine placement within the search region. Specifically, the frequency of occurrence of the event that a mine exists in the cell and is not detected is recorded for each grid cell. Hence, both placement and detection events require recording, with the cell-specific event occurrence given by the ratio of placement to detection events. For this experiment, it is necessary that the test statistic not be dependent on the actual number of occurrences. Otherwise, it would depend on the number of realizations and not be a valid context for the experiment. The cell-specific occurrences are averaged over the grid and the results plotted in figure 22.

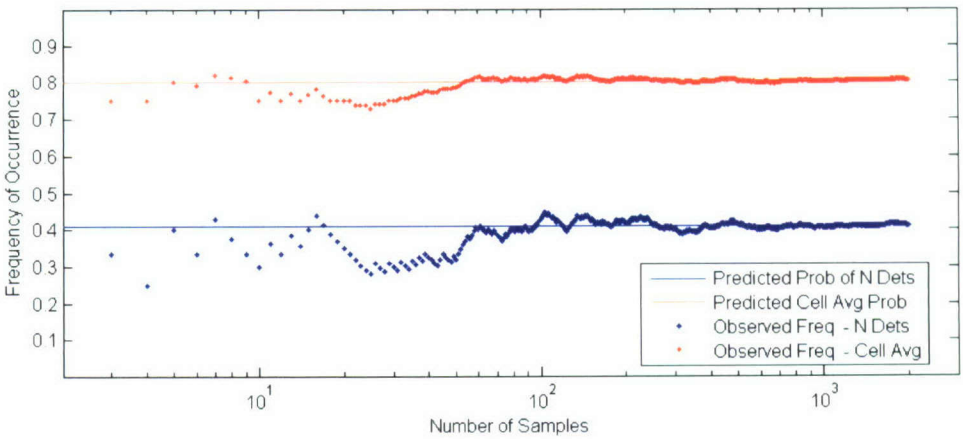

Figure 22. Clearance Event Frequency of Occurrence

The convergence of the observed experimental frequencies of occurrence to their predicted probabilities is apparent in figure 22. The achieved tolerances exhibited in figures 21 and 22 remain to be articulated, however. What is important to observe is the difference in the performance assessments themselves. The search effort evaluation presented in the cell average probability corresponds to a blind search where it is unclear what the actual context is and, hence, precisely what it is that you are looking for. As this measure is developed over the probability density function extracted from the mine density λ-decomposition, a single mine context applies. Thus, the result provides a probability that if a single mine were present in the region, it would be detected. For this case where detection probability P_D and mine density λ are constant over the region, it becomes equivalent to the sensor characterization independent of geography. Note that this will not generally be the case. The probability of detecting all mines in a search region presents a more stringent criterion to meet—it is contingent on having that precise knowledge in forming the evaluation metric. For this case, the search is presumably highly directed and search effort applied until all mines have been detected to within a specified probability. For the single area sweep presented in figure 22, the predicted probability of finding four mines is 0.4096. This contrasts with a search effort threshold of 0.8 that was applied. In comparison, a P_{SS} next detection probability calculation using an expected number of mines of $N_M = 1$ yields a predicted value of 0.5507.

The remaining experiments are conducted using non-uniform mine and clutter densities. In addition, a field structure is applied in developing the mine density function. For these experiments, the mine field consists of a single line with 12 possible mine locations along the line. The expected number of mines populating the field is set to four. A random mine placement is also applied with an expected number of two, yielding a total expected number of six mines placed in the search region. These numbers are kept artificially low so as to extend the partial search path before a P_{SS} threshold criterion of 0.8 is met, as the intent is to demonstrate the properties of the search evaluation capability. The partial search path where this condition is met is depicted in figure 23. Also shown are contours corresponding to the respective mine and clutter density functions.

To emulate mine classification degradation in the presence of clutter, an artificial reduction in detection probability in the form of

$$P_D(\mathbf{x}) = 0.8 - 0.2 \cdot \lambda_C(\mathbf{x}) / \lambda_{C\max} \tag{111}$$

is introduced to yield an unweighted average P_D of 0.764 over the space and a density weighted average of 0.732. The combination of spatial variability and mine field structure results in the predicted probabilities shown in figure 24. The impact of spatial variability on the next detection probabilities relative to that of the baseline P_{SS} (recall that the baseline is conditioned on a uniform distribution) is readily apparent for this partial search path. The separation between the next detection probabilities assuming a known or unknown number of mines is less apparent than in figure 20. This is due to the increase in the expected number of total mines in the search space. In general, the next detection probability curves for a known and unknown number of mines converge as the expected number of mines N_M increases.

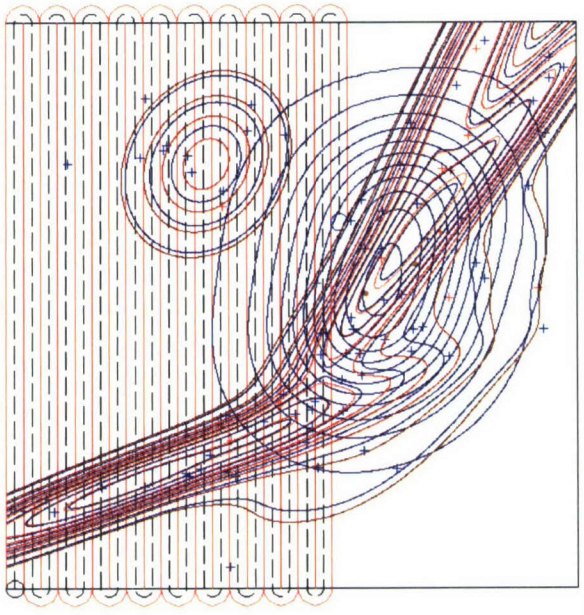

Figure 23. Structured Drop Experiment Mine and Clutter Densities

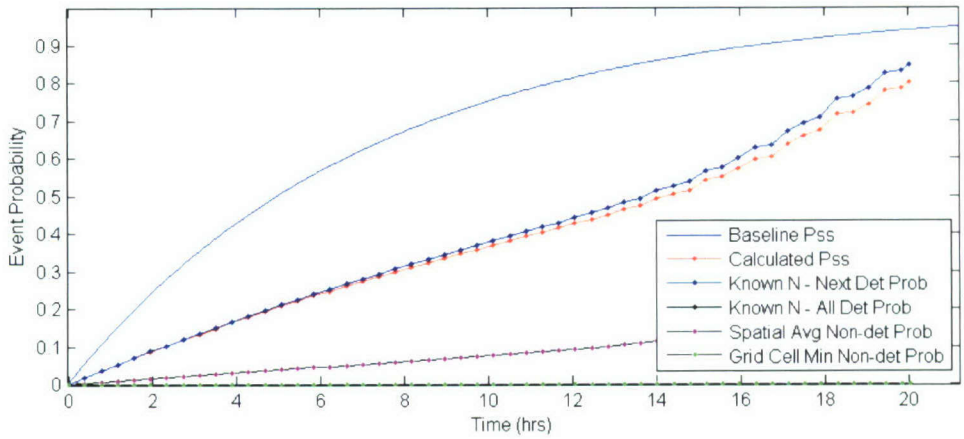

Figure 24. Structured Drop Experiment Predicted Probabilities

Figure 25 illustrates the results of a simulation conducted to demonstrate anticipated mine detections versus detections due to false alarm clutter. The clutter density spatial Poisson process is colored by a value of $P_C = 0.85$, denoting the probability of classifying the clutter properly. The unclassified clutter forms an independent spatial Poisson process, and the detection of these mine-like objects constitutes a false alarm. Figure 25 plots the ensemble average of the number of detections occurring along a partial search path that is terminated when the false alarm probability reaches a value of 0.8.

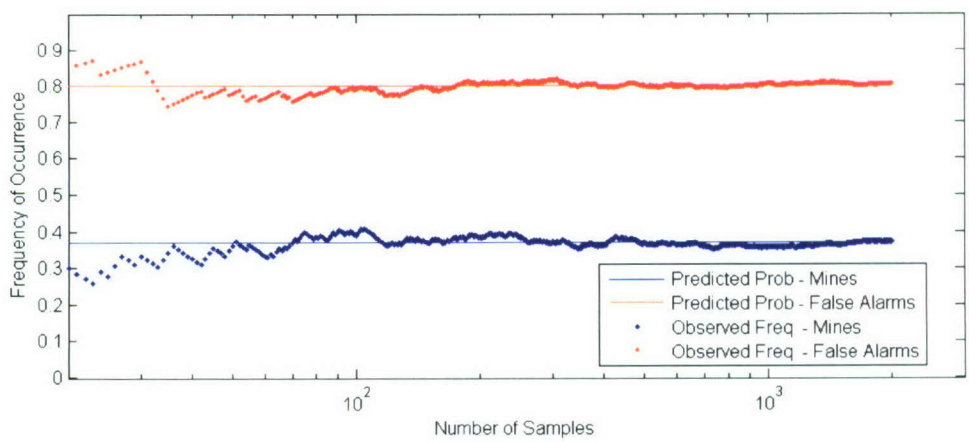

Figure 25. Detection and False Alarm Frequency of Occurrence

The expected values of the number of mine detections and false alarms encountered along the search path provide additional criteria in comparing search paths under geometrically varying conditions. Figure 26 shows the evolution of the expectations as the search path is executed. The end-case ensemble of 2000 simulation runs was used in constructing this figure. For this depiction, one complete sweep of the search region is executed. The figure shows the calculated expected values, the average of the number of observed detections that occur for each time step, and a set of bounds corresponding to the standard deviation of the ensemble. For this example, the results demonstrate the dependency on spatial variability and the richness of the false alarm density relative to that of the mine density.

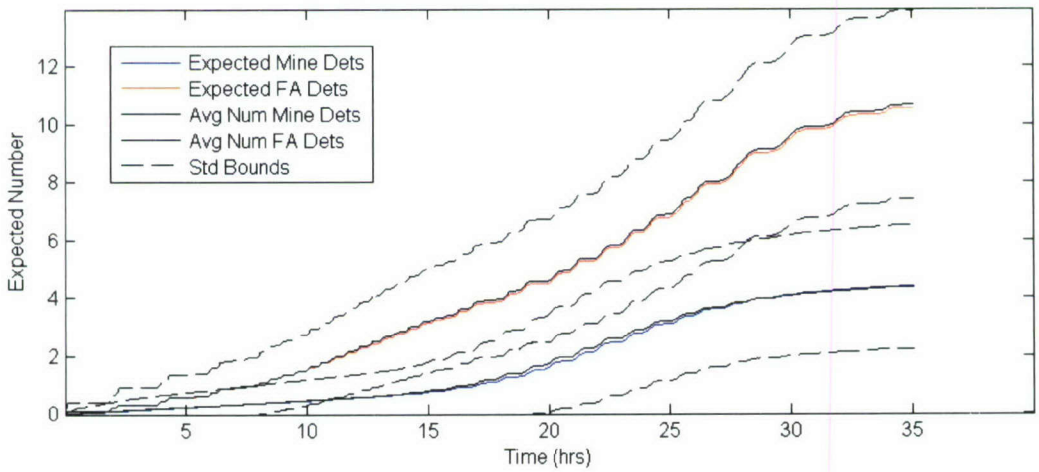

Figure 26. Expected Number of Detections and False Alarms

5. SUMMARY AND FUTURE WORK

This report has detailed the development of a search path evaluation capability for objects that may be placed with spatial structure, such as occurs in mine-hunting applications. The method is based on a rigorous extension of previous work on distributed search theory, whereby searcher motion is combined with spatial patterns of the objects of search. This probabilistic view of the spatio-temporal search process is consistent with uncertainty representations that are characteristic of information provided for the assessment of realistic mine-hunting operations. The method is appropriate for objects occurring randomly or in spatial patterns, for a known or unknown number of objects, and with or without clutter contacts. Furthermore, the method works with search paths of arbitrary complexity, including search paths that self-intersect.

In the process of developing this capability, a significant degree of mathematical rigor was applied to create the event spaces over which probabilistic calculations are based. As a consequence, several maps were developed either on the global search region scale or on the local sensor referenced subspace. These include the respective mine and clutter density maps, the detection and non-detection probability maps, and the respective mine field maps associated with a reference placement of an identified mine. These maps are a byproduct of the search evaluation procedure; yet, they may prove to be useful as additional information to an operator. The cases of prior knowledge on the number of mines in the search environment or its expected value were considered. When mine field structure is assumed, the actual or expected value of the number of mine fields is applied as well. A variety of performance results were developed and presented to clarify the capability in terms of its functionality, efficacy, and accuracy.

The numerical procedure for search evaluation employs a grid-based realization so as to readily incorporate environmental influences on mine placement and the spatial characterization of clutter. Additionally, the capability integrates a degree of prior knowledge on mine field structure into the evaluation methodology. This modeled structure is incorporated into calculation of the probability of finding the next mine for the cases of no identified mines or a spatially diverse set of known identifications. The method is based on a notion of search effort swept over time, so it is directly applicable to any sensing modality that can be represented as a probability over range in directions relative to searcher motion. This search evaluation capability does not address the fusion of prior knowledge of mine field structure with the location of multiple identified mines within mine field proximity to each other. It can incorporate such output from algorithms that do perform fusion on multiple observations if it is provided in the prior knowledge specification.

While the method is appropriate for robust computation of problems of current interest, there are a number of extensions that can improve the capability. The tessellation of the search space (to represent underlying mine and clutter density functions) was limited to square grids for ease of development. There are many alternate tessellations, both uniform (such as hexagons) and non-uniform (such as different sized rectangles), that may prove to be computationally advantageous. As the problem scale increases, this is an area that may merit consideration. Another computational complexity issue is to determine the appropriate tradeoffs between

effectiveness of computation and speed of computation, which can be computed as a function of grid evaluation parameters using available Pareto optimization techniques (reference 13).

With respect to the search path input, the method currently assumes a perfectly known search path, with uniformly sampled time intervals. Obviously, time sampling can be applied to any given path to meet the uniform sampling intervals, but that may also prove to be computationally inefficient, especially for search paths that have extended periods of non-maneuvering. Finally, the search paths are assumed to be known precisely; assessment of search effectiveness under the anticipated uncertainty in navigational accuracy of the search platform is of critical importance. Since the search effectiveness is based on probability representations of searcher performance, the effects of positional uncertainty of the searcher are regularly incorporated into the method; this is a subject of current investigation.

Future extensions of this search evaluation capability include the development of additional probability metrics for search evaluation beyond probability of successful search. Of primary importance in the mine-hunting application is the representation of the probability of obtaining queue roots that provide a mine-free (within some pre-determined certainty) path of given width but arbitrary shape between two points. A direct extension of this method is to multiple searchers, as the maps that underlie the search computations can be updated simultaneously for any number of collaborating searchers. The impact of data fusion between such searchers is also a simple extension, given a known description of the impact of the fusion process on the corresponding P_D values.

The initial uses of this search evaluation capability include the determination of effectiveness inside of various path optimization strategies. Such applications will take advantage of the robust computational nature of the approach. The evaluation of various competing fusion strategies for multiple searcher mine hunting is another initial area of use. Other intended uses include the development of new displays that represent regularly updated mine location likelihood maps as search progresses. Within the operational community, the search evaluation capability can be used to determine the impact on search evaluation obtained by providing more (or less) information about the expected mine field characteristics. All of these applications are under consideration.

6. REFERENCES

1. T. A. Wettergren, "Statistical Analysis of Detection Performance for Large Distributed Sensor Systems," NUWC-NPT Technical Report 11,436, Naval Undersea Warfare Center Division, Newport, RI, June 2003.

2. T. A. Wettergren, "Performance of Search Via Track-Before-Detect for Distributed Sensor Networks," to appear in *IEEE Transactions on Aerospace and Electronic Systems*.

3. B. G. Koopman, *Search and Screening: General Principles and Historical Applications*, Pergamon Press, New York, 1980.

4. A. R. Washburn, *Search and Detection*, 4th Edition, INFORMS, Linthicum, MD, 2002.

5. L. D. Stone, *Theory of Optimal Search*, 2nd Edition, ORSA Books, Arlington, VA, 1989.

6. K. Iida, *Studies on the Optimal Search Plan*, Springer-Verlag, Berlin, 1992.

7. D. Grace, "Brownian Reber Search Theory for the Advanced Unmanned Search System (AUSS), NCCOSC Technical Report 1534, Naval Command, Control, and Ocean Surveillance Center, San Diego, CA, October 1992.

8. G. R. Grimmett and D. R. Stirzaker, *Probability and Random Processes*, Oxford University Press, New York, 2001.

9. A. Papoulis, *Probability, Random Variables, and Stochastic Processes*, Third Edition, McGraw-Hill, Boston, 1991.

10. J. F. C. Kingman, *Poisson Processes*, Oxford University Press, New York, 1995.

11. L. D. Stone, J. A. Stanshine, and C. A. Persinger, "Optimal Search in the Presence of Poisson-Distributed False Targets," *SIAM Journal on Applied Mathematics*, vol. 23, no. 1, 1972, pp. 6-27.

12. A. Caticha and R. Preuss, "Maximum Entropy and Bayesian Data Analysis: Entropic Prior Distributions," *Physical Review E*, vol. 70, 046127 (2004).

13. T. A. Wettergren, "The Genetic-Algorithm-Based Normal Boundary Intersection (GANBI) Method: An Efficient Approach to Pareto Multiobjective Optimization for Engineering Design," NUWC-NPT Technical Report 11,741, Naval Undersea Warfare Center Division, Newport, RI, May 2006.

14. R. Durrett, *Probability: Theory and Examples*, Brooks/Cole-Thomson Learning, Belmont, CA, 2005.

15. W. L. Brogan, *Modern Control Theory*, Second Edition, Prentice-Hall, Englewood Cliffs, NJ, 1985.

APPENDIX A
PROBABILITY BACKGROUND

A.1 REVIEW OF PROBABILITY SPACES

A *probability space* represented by the triple $(\Omega, \mathcal{F}, P)$ comprises a totally finite *measure space*, with P denoting a probability measure (references 8 and 14). Here, Ω denotes the set of possibilities under consideration, $\mathcal{F}$ denotes an event space consisting of a collection of selected subsets of Ω, and the probability measure P: $\mathcal{F} \rightarrow [0, 1]$ realizes a set function mapping events $E \in \mathcal{F}$ to numbers denoting the likelihood of event occurrence. The set Ω is often described as the set of possible outcomes of some experiment where Ω is exclusive and exhaustive; that is, outcomes can consist of only one member of the set and no other outcomes of the experiment are possible. In contrast, events often consist of a set of outcomes and the event space may, or may not, include individual outcomes as *singleton* events.

For $\mathcal{F}$ to be a valid event space, $\mathcal{F}$ must comprise a σ-algebra and every element of $\mathcal{F}$ must be P-measurable. For any collection $\mathcal{F} \subseteq \mathcal{P}(\Omega)$, where $\mathcal{P}(\Omega)$ represents the power set of all possible subsets of Ω, $\mathcal{F}$ is a σ-algebra if and only if:

(i) $\phi \in \mathcal{F}$.

(ii) If $E \in \mathcal{F}$, then $\sim E \in \mathcal{F}$.

(iii) For any countable sequence $\langle E_i \rangle_{i=1}^{\infty}$ of elements of $\mathcal{F}$,

$$\bigcup_{i=1}^{\infty} E_i \in \mathcal{F}.$$

In the above, $\sim E$ denotes the set complement of E with respect to Ω, and ϕ is the empty set. As ϕ must be in the event space, so must be its complement Ω. Also, from (ii) and (iii), all countable intersections of events must be in the event space. If $\mathcal{F}$ is a valid σ–algebra, then $(\Omega, \mathcal{F})$ is a measurable space. For P to be a valid measure on $(\Omega, \mathcal{F})$, the following must hold:

(i) $P(\phi) = 0$.

(ii) $P(E) \geq 0$ for all $E \subseteq \mathcal{F}$.

(iii) For any countable sequence $\langle E_i \rangle_{i=1}^{\infty}$ of elements of $\mathcal{F}$ where the E_i are disjoint,

$$P\left(\bigcup_{i=1}^{\infty} E_i\right) = \sum_{i=1}^{\infty} P(E_i).$$

If these conditions are met, the triple $(\Omega, \mathcal{F}, P)$ is called a measure space. The measure space becomes a probability space when $P(\Omega) = 1$, with P being a probability measure.

Observe that the smallest possible event space (i.e., σ–algebra) consists of the set $\{\phi, \Omega\}$. However, this σ–algebra is non-informative and no probability questions regarding a particular subset of Ω can be asked. What is important for purposes of search path evaluation is that event spaces are constructed that are specific to the set of probability questions to be answered. That is, given a probability question (e.g., the probability of finding a mine along a given search path within a specific interval of time), an event space $\mathcal{F}$ is constructed that yields the smallest σ–algebra necessary to answer the question.

A.2 REVIEW OF SPATIAL POISSON PROCESSES

The spatial Poisson process is a multi-dimensional extension of the set of arrival times associated with a one-dimensional Poisson process. For our purposes, the arrival characteristic concerns the placement of objects in a two-dimensional space. Objects persist in the space, so the experimental outcome occurs only once. However, given any arbitrary region $A \subseteq S$, the number of objects occurring in that region of the search space N(A) becomes a Poisson distributed random variable. The details of this process are given below.

Let A be a collection of Lebesgue measurable* regions $\{A\}_{A \in A}$ within the search space S. Then, $\{N(A)\}_{A \in A}$ is a *homogeneous* spatial Poisson point process with constant intensity λ if:

(i) For each $A \in A$, $N(A) \sim \text{Poisson}(\lambda|A|)$.

(ii) For every finite collection $\{A_1, A_2, \ldots, A_n\}$ of disjoint subsets of S, $N(A_1), N(A_2), \ldots, N(A_n)$ are independent random variables.

There are alternate axiomatic conditions that the spatial Poisson process satisfies. These are:

(i) If $A_1, A_2, \ldots, A_n$ are disjoint regions, then $N(A_1), N(A_2), \ldots, N(A_n)$ are independent random variables and
$$N\left(\bigcup_{i=1}^{n} A_i\right) = \sum_{i=1}^{n} N(A_i).$$

(ii) The probability distribution of N(A) depends on set A only through its size |A|.

(iii) There is zero probability of points overlapping:
$$\lim_{|A| \to 0} \frac{\Pr(N(A) \geq 1)}{\Pr(N(A) = 1)} = 1.$$

Then, for any spatial region $A \subseteq S$, the probability of finding k objects within A for $k = 0, 1, 2, \ldots$, is

*Any countable union of intervals in P, or rectangles in P^2, is Lebesgue measurable.

$$\Pr(N(A) = k) = \frac{(\lambda|A|)^k}{k!} \exp(-\lambda|A|).$$

Next, the requirement of using a Lebesgue measure on P^2 is relaxed and variability of the intensity parameter λ over the search space S is allowed. Let

$$\Lambda(A) = \int_A \lambda(x)\,dx$$

for all Lebesgue measurable $A \subseteq S$. Denote the set function $\Lambda(A)$ as the mean measure of A and variable λ as a characterization of a *non-homogeneous* spatial Poisson process.*

The axiomatic requirements for such a process become:

(i) For each $A \in A$, $N(A) \sim \text{Poisson}(\Lambda(A))$.

(ii) For every finite collection $\{A_1, A_2, \ldots, A_n\}$ of disjoint subsets of S, $N(A_1), N(A_2), \ldots, N(A_n)$ are independent random variables.

Two important theorems regarding spatial Poisson processes of particular relevance to search path evaluation are stated here in terse form and without proof. Readers can refer to reference 8 for a more complete coverage of the topics.

Superposition Theorem: Let Π_1 and Π_2 be independent spatial Poisson processes with intensity functions λ_1 and λ_2. Then, the set $\Pi = \Pi_1 \cap \Pi_2$ is a spatial Poisson process with intensity function $\lambda = \lambda_1 + \lambda_2$.

Coloring Theorem: Let Π be a *non-homogeneous* spatial Poisson process with intensity function $\lambda(x)$. Let each point of Π be "colored" independently as green at x with probability $\gamma(x)$ and red with probability $\rho(x) = 1 - \gamma(x)$. Let Γ and P be the set of points that are colored green and red. Then, Γ and P are independent spatial Poisson processes with respective intensity functions $\gamma(x)\lambda(x)$ and $\rho(x)\lambda(x)$.

These properties and theorems allow the construction of mine density functions and sensory characterizations that vary over the search space. To show this, let $\lambda(x)$ be a mine density function (i.e., intensity) associated with a spatial Poisson process Π. Then, for each point of Π, let Π_P be the occurrences colored by the detection event, with probability $P_D(x)$, and let Π_Q be the occurrences colored by non-detection, with probability $Q_D(x) = 1 - P_D(x)$. Then, from the above theorems, Π_P and Π_Q constitute independent spatial Poisson processes with respective density functions $P_D(x)\lambda(x)$ and $(1 - P_D(x))\lambda(x)$.

---

*Note that when λ is constant, $\Lambda(A) = \int_A \lambda\,dx = \lambda \int_A dx = \lambda|A|$.

APPENDIX B
JOINT DENSITY DEVELOPMENT FOR GAUSSIAN FIELDS

This appendix provides the development for the joint probability density function discussed in section 2.2 for the case of a field structure comprising Gaussian components. Each structure component is modeled as a normally distributed random variable $\mathbf{x}_j$, $j = 1, \ldots, N_M$ placed about the common reference point $\mathbf{x}_{ref}$ in the search space $S \subseteq R^2$. Let $\hat{\mathbf{x}}_j = \mathbf{x}_{ref} + \Delta\mathbf{x}_j$ designate the intended position of object m_j with displacement $\Delta\mathbf{x}_j$ from the reference. Let each reference conditional placement be distributed as $\mathbf{x}_j \sim N[\hat{\mathbf{x}}_j, \mathbf{I}_2\sigma_p^2]$ and assume that tail probability outside S is negligible. As shown in equation (49), the joint conditional density takes the form

$$\begin{aligned} f(\mathbf{x}_1,\ldots,\mathbf{x}_{N_M} \mid \mathbf{x}_{ref}) &= \prod_{j=1}^{N_M} f_j(\mathbf{x}_j \mid \mathbf{x}_{ref}), \\ &= \left[2\pi\sigma_P^2\right]^{-N_M} \exp\left[-\frac{1}{2\sigma_P^2}\sum_{j=1}^{N_M}\left((x_j-\hat{x}_j)^2+(y_j-\hat{y}_j)^2\right)\right]. \end{aligned} \tag{B-1}$$

Let the field placement density also be Gaussian, $\mathbf{x}_{ref} \sim N[\hat{\mathbf{x}}_0, \mathbf{I}_2\sigma_{ref}^2]$. Then, the unconditional joint density can be developed via marginalization as in equation (41). This development is tedious, however, and it is more insightful to map the conditional density into a form where the unconditional joint density is readily recognized, as in

$$f(\mathbf{x}_1,\ldots,\mathbf{x}_{N_M},\mathbf{x}_{ref}) = f(\mathbf{x}_{ref} \mid \mathbf{x}_1,\ldots,\mathbf{x}_{N_M}) \cdot f(\mathbf{x}_1,\ldots,\mathbf{x}_{N_M}). \tag{B-2}$$

Here, $f(\mathbf{x}_{ref} \mid \mathbf{x}_1,\ldots,\mathbf{x}_{N_M})$ represents the posterior probability density function of where the reference point may be located given the field placement prior and independent observations of the N_M distinct objects in the structure. The notation $\mathbf{z}_j = \mathbf{x}_j - \Delta\mathbf{x}_j = \mathbf{x}_{ref} + \mathbf{n}_j$ is used to denote observations on reference location, with $\mathbf{n}_j \sim N[\mathbf{0}, \mathbf{I}_2\sigma_p^2]$ as above. Let

$$\mathbf{Z} = \left[\mathbf{z}_1, \mathbf{z}_2, \ldots, \mathbf{z}_{N_M}\right]^T = \mathbf{A} \cdot \mathbf{x}_{ref} + \left[\mathbf{n}_1, \mathbf{n}_2, \ldots, \mathbf{n}_{N_M}\right]^T \tag{B-3}$$

denote the vector of such observations with $\mathbf{A} = \left[\mathbf{I}_2, \mathbf{I}_2, \ldots, \mathbf{I}_2\right]^T$ and covariance matrix $\mathbf{R}_z = \sigma_p^2 \cdot \mathbf{I}_{2N_M}$. Then, the reference conditional and prior densities take the form

$$f(\mathbf{x}_1,\ldots,\mathbf{x}_{N_M} \mid \mathbf{x}_{ref}) = \frac{1}{\left[2\pi\sigma_p^2\right]^{N_M}} \exp\left(-\frac{1}{2}\left[\mathbf{Z}-\mathbf{A}\mathbf{x}_{ref}\right]^T \mathbf{R}_z^{-1}\left[\mathbf{Z}-\mathbf{A}\mathbf{x}_{ref}\right]\right), \tag{B-4}$$

$$f(\mathbf{x}_{ref}) = \frac{1}{2\pi\sigma_{ref}^2} \exp\left(-\frac{1}{2}\left[\mathbf{x}_0-\mathbf{x}_{ref}\right]^T \mathbf{R}_0^{-1}\left[\mathbf{x}_0-\mathbf{x}_{ref}\right]\right), \tag{B-5}$$

where $\mathbf{R}_0 = \sigma_{ref}^2 \cdot \mathbf{I}_2$. The joint density, including field and object placement, becomes

$$f(\mathbf{x}_1,\ldots,\mathbf{x}_{N_M},\mathbf{x}_{ref}) = \frac{1}{\left[2\pi\sigma_p^2\right]^{N_M} 2\pi\sigma_{ref}^2}\exp\left(-\frac{1}{2}\left[\mathbf{Z}-\mathbf{A}\mathbf{x}_{ref}\right]^T\mathbf{R}_z^{-1}\left[\mathbf{Z}-\mathbf{A}\mathbf{x}_{ref}\right]-\frac{1}{2}\left[\mathbf{x}_0-\mathbf{x}_{ref}\right]^T\mathbf{R}_0^{-1}\left[\mathbf{x}_0-\mathbf{x}_{ref}\right]\right). \quad \text{(B-6)}$$

Let L denote the exponent of equation (B-6) without the scalar term, -1/2. Then,

$$\begin{aligned} L &= \left[\mathbf{Z}-\mathbf{A}\mathbf{x}_{ref}\right]^T\mathbf{R}_z^{-1}\left[\mathbf{Z}-\mathbf{A}\mathbf{x}_{ref}\right]+\left[\mathbf{x}_0-\mathbf{x}_{ref}\right]^T\mathbf{R}_0^{-1}\left[\mathbf{x}_0-\mathbf{x}_{ref}\right], \\ &= \mathbf{x}_{ref}^T\left[\mathbf{R}_0^{-1}+\mathbf{A}^T\mathbf{R}_z^{-1}\mathbf{A}\right]\mathbf{x}_{ref}-2\mathbf{x}_{ref}^T\left[\mathbf{R}_0^{-1}\mathbf{x}_0+\mathbf{A}^T\mathbf{R}_z^{-1}\mathbf{Z}\right]+\mathbf{Z}^T\mathbf{R}_z^{-1}\mathbf{Z}+\mathbf{x}_0^T\mathbf{R}_0^{-1}\mathbf{x}_0. \end{aligned} \quad \text{(B-7)}$$

With $\rho_p = \sigma_p/\sigma_{ref}$ and following the standard development in reference 15, the notation

$$\begin{aligned} \mathbf{P}_{x/z}^{-1} &= \mathbf{R}_0^{-1}+\mathbf{A}^T\mathbf{R}_z^{-1}\mathbf{A}, \\ &= \frac{1}{\sigma_{ref}^2}\mathbf{I}_2+\sum_{j=1}^{N_M}\frac{1}{\sigma_p^2}\mathbf{I}_2 = \frac{N_M\sigma_{ref}^2+\sigma_p^2}{\sigma_{ref}^2\sigma_p^2}\mathbf{I}_2 = \frac{N_M+\rho_p^2}{\sigma_p^2}\mathbf{I}_2, \end{aligned} \quad \text{(B-8)}$$

$$\begin{aligned} \hat{\mathbf{x}}_{ref} &= \left[\mathbf{R}_0^{-1}+\mathbf{A}^T\mathbf{R}_z^{-1}\mathbf{A}\right]^{-1}\left[\mathbf{R}_0^{-1}\mathbf{x}_0+\mathbf{A}^T\mathbf{R}_z^{-1}\mathbf{Z}\right], \\ &= \frac{\sigma_p^2}{N_M+\rho_p^2}\left[\frac{1}{\sigma_{ref}^2}\mathbf{x}_0+\sum_{j=1}^{N_M}\frac{1}{\sigma_p^2}\mathbf{z}_j\right] = \frac{\rho_p^2}{N_M+\rho_p^2}\mathbf{x}_0+\frac{N_M}{N_M+\rho_p^2}\left[\frac{1}{N_M}\sum_{j=1}^{N_M}\left(\mathbf{x}_j-\Delta\mathbf{x}_j\right)\right], \end{aligned} \quad \text{(B-9)}$$

is used to denote the respective information matrix and conditional mean of the reference posterior density $f(\mathbf{x}_{ref} \mid \mathbf{x}_1,\ldots,\mathbf{x}_{N_M})$. Completing the square in equation (B-7) yields

$$\begin{aligned} L &= \mathbf{x}_{ref}^T\mathbf{P}_{x/z}^{-1}\mathbf{x}_{ref}-2\mathbf{x}_{ref}^T\mathbf{P}_{x/z}^{-1}\hat{\mathbf{x}}_{ref}+\mathbf{Z}^T\mathbf{R}_z^{-1}\mathbf{Z}+\mathbf{x}_0^T\mathbf{R}_0^{-1}\mathbf{x}_0, \\ &= \left[\mathbf{x}_{ref}-\hat{\mathbf{x}}_{ref}\right]^T\mathbf{P}_{x/z}^{-1}\left[\mathbf{x}_{ref}-\hat{\mathbf{x}}_{ref}\right]+\mathbf{Z}^T\mathbf{R}_z^{-1}\mathbf{Z}+\mathbf{x}_0^T\mathbf{R}_0^{-1}\mathbf{x}_0-\hat{\mathbf{x}}_{ref}^T\mathbf{P}_{x/z}^{-1}\hat{\mathbf{x}}_{ref}. \end{aligned} \quad \text{(B-10)}$$

That part of L that does not correspond to the reference point posterior becomes

$$\begin{aligned} L_z &= \mathbf{Z}^T\mathbf{R}_z^{-1}\mathbf{Z}+\mathbf{x}_0^T\mathbf{R}_0^{-1}\mathbf{x}_0-\hat{\mathbf{x}}_{ref}^T\mathbf{P}_{x/z}^{-1}\hat{\mathbf{x}}_{ref}, \\ &= \mathbf{Z}^T\mathbf{R}_z^{-1}\mathbf{Z}+\mathbf{x}_0^T\mathbf{R}_0^{-1}\mathbf{x}_0-\left[\mathbf{R}_0^{-1}\mathbf{x}_0+\mathbf{A}^T\mathbf{R}_z^{-1}\mathbf{Z}\right]^T\mathbf{P}_{x/z}\left[\mathbf{R}_0^{-1}\mathbf{x}_0+\mathbf{A}^T\mathbf{R}_z^{-1}\mathbf{Z}\right], \\ &= \mathbf{Z}^T\left[\mathbf{R}_z^{-1}-\mathbf{R}_z^{-1}\mathbf{A}\mathbf{P}_{x/z}\mathbf{A}^T\mathbf{R}_z^{-1}\right]\mathbf{Z}-2\mathbf{Z}^T\mathbf{R}_z^{-1}\mathbf{A}\mathbf{P}_{x/z}\mathbf{R}_0^{-1}\mathbf{x}_0+\mathbf{x}_0^T\left[\mathbf{R}_0^{-1}-\mathbf{R}_0^{-1}\mathbf{P}_{x/z}\mathbf{R}_0^{-1}\right]\mathbf{x}_0. \end{aligned} \quad \text{(B-11)}$$

To complete the square in **Z**, let

$$\begin{aligned} \mathbf{P}_z^{-1} &= \mathbf{R}_z^{-1}-\mathbf{R}_z^{-1}\mathbf{A}\mathbf{P}_{x/z}\mathbf{A}^T\mathbf{R}_z^{-1}, \\ &= \frac{1}{\sigma_p^2}\mathbf{I}_{2N_M}-\frac{1}{\sigma_p^2}\frac{\sigma_{ref}^2\sigma_p^2}{N_M\sigma_{ref}^2+\sigma_p^2}\frac{1}{\sigma_p^2}\mathbf{A}\mathbf{A}^T = \frac{1}{\sigma_p^2}\left[\mathbf{I}_{2N_M}-\frac{\sigma_{ref}^2}{N_M\sigma_{ref}^2+\sigma_p^2}\mathbf{A}\mathbf{A}^T\right] \end{aligned} \quad \text{(B-12)}$$

denote the information matrix of the marginalized density. Covariance matrix $\mathbf{P}_z$ is readily obtained by applying the matrix inversion lemma to equation (B-12) and simplifying terms. Doing so, one obtains

$$\begin{aligned}\mathbf{P}_z &= \mathbf{R}_z + \mathbf{A}\left[\mathbf{P}_{x/z}^{-1} - \mathbf{A}^T\mathbf{R}_z^{-1}\mathbf{A}\right]^{-1}\mathbf{A}^T = \mathbf{R}_z + \mathbf{A}\mathbf{R}_0\mathbf{A}^T, \\ &= \sigma_p^2\mathbf{I}_{2N_M} + \sigma_{ref}^2\mathbf{A}\mathbf{A}^T.\end{aligned} \tag{B-13}$$

Using this form, the marginalized density mean value simplifies accordingly to

$$\begin{aligned}\hat{\mathbf{Z}} &= \left[\mathbf{R}_z^{-1} - \mathbf{R}_z^{-1}\mathbf{A}\mathbf{P}_{x/z}\mathbf{A}^T\mathbf{R}_z^{-1}\right]^{-1}\left[\mathbf{R}_z^{-1}\mathbf{A}\mathbf{P}_{x/z}\mathbf{R}_0^{-1}\mathbf{x}_0\right], \\ &= \left[\sigma_p^2\mathbf{I}_{2N_M} + \sigma_{ref}^2\mathbf{A}\mathbf{A}^T\right]\frac{1}{\sigma_p^2}\frac{\sigma_p^2}{N_M+\rho_p^2}\frac{1}{\sigma_{ref}^2}\mathbf{A}\mathbf{x}_0, \\ &= \left[\frac{\rho_p^2}{N_M+\rho_p^2}\mathbf{A} + \frac{1}{N_M+\rho_p^2}\mathbf{A}\mathbf{A}^T\mathbf{A}\right]\mathbf{x}_0 = \mathbf{A}\mathbf{x}_0,\end{aligned} \tag{B-14}$$

where the substitution $\mathbf{A}^T\mathbf{A} = N_M\mathbf{I}_2$ has been used. Completing the square yields

$$L_z = \left[\mathbf{Z} - \hat{\mathbf{Z}}\right]^T\mathbf{P}_z^{-1}\left[\mathbf{Z} - \hat{\mathbf{Z}}\right] + \mathbf{x}_0^T\left[\mathbf{R}_0^{-1} - \mathbf{R}_0^{-1}\mathbf{P}_{x/z}\mathbf{R}_0^{-1}\right]\mathbf{x}_0 - \hat{\mathbf{Z}}^T\mathbf{P}_z^{-1}\hat{\mathbf{Z}}. \tag{B-15}$$

Rearranging equation (B-8) and substituting $\mathbf{A}^T\mathbf{R}_z^{-1}\mathbf{A} = \mathbf{P}_{x/z}^{-1} - \mathbf{R}_0^{-1}$,

$$\begin{aligned}&\mathbf{x}_0^T\left[\mathbf{R}_0^{-1} - \mathbf{R}_0^{-1}\mathbf{P}_{x/z}\mathbf{R}_0^{-1}\right]\mathbf{x}_0 - \hat{\mathbf{Z}}^T\mathbf{P}_z^{-1}\hat{\mathbf{Z}}, \\ &= \mathbf{x}_0^T\left[\mathbf{R}_0^{-1} - \mathbf{A}^T\mathbf{R}_z^{-1}\mathbf{A} - \mathbf{R}_0^{-1}\mathbf{P}_{x/z}\mathbf{R}_0^{-1} + \mathbf{A}^T\mathbf{R}_z^{-1}\mathbf{A}\mathbf{P}_{x/z}\mathbf{A}^T\mathbf{R}_z^{-1}\mathbf{A}\right]\mathbf{x}_0, \\ &= \mathbf{x}_0^T\left[\mathbf{R}_0^{-1} - \mathbf{A}^T\mathbf{R}_z^{-1}\mathbf{A} - \mathbf{R}_0^{-1}\mathbf{P}_{x/z}\mathbf{R}_0^{-1} + \left[\mathbf{P}_{x/z}^{-1} - \mathbf{R}_0^{-1}\right]\mathbf{P}_{x/z}\mathbf{A}^T\mathbf{R}_z^{-1}\mathbf{A}\right]\mathbf{x}_0, \\ &= \mathbf{x}_0^T\left[\mathbf{R}_0^{-1} - \mathbf{R}_0^{-1}\mathbf{P}_{x/z}\mathbf{R}_0^{-1} - \mathbf{R}_0^{-1}\mathbf{P}_{x/z}\mathbf{A}^T\mathbf{R}_z^{-1}\mathbf{A}\right]\mathbf{x}_0, \\ &= \mathbf{x}_0^T\left[\mathbf{R}_0^{-1} - \mathbf{R}_0^{-1}\mathbf{P}_{x/z}\left[\mathbf{R}_0^{-1} + \mathbf{A}^T\mathbf{R}_z^{-1}\mathbf{A}\right]\right]\mathbf{x}_0, \\ &= \mathbf{x}_0^T\left[\mathbf{R}_0^{-1} - \mathbf{R}_0^{-1}\right]\mathbf{x}_0, \\ &= 0.\end{aligned} \tag{B-16}$$

Hence,

$$L_z = \left[\mathbf{Z} - \mathbf{A}\mathbf{x}_0\right]^T\mathbf{P}_z^{-1}\left[\mathbf{Z} - \mathbf{A}\mathbf{x}_0\right]. \tag{B-17}$$

To return the exponent to an expression in the respective $\mathbf{x}_j$, recall that $\mathbf{z}_j = \mathbf{x}_j - \Delta\mathbf{x}_j$. Let the vector of object positions and mean values be defined as

$$\mathbf{X} = \left[\mathbf{x}_1, \mathbf{x}_2, \ldots, \mathbf{x}_{N_M}\right]^T, \quad \hat{\mathbf{X}} = \left[\mathbf{x}_0 + \Delta\mathbf{x}_1, \mathbf{x}_0 + \Delta\mathbf{x}_2, \ldots, \mathbf{x}_0 + \Delta\mathbf{x}_{N_M}\right]^T. \tag{B-18}$$

Then, the quadratic form in equation (B-17) is equivalent to

$$L_z = \left[\mathbf{X} - \hat{\mathbf{X}}\right]^T \mathbf{P}_z^{-1} \left[\mathbf{X} - \hat{\mathbf{X}}\right]. \tag{B-19}$$

It remains to show that the normalizing factors associated with the reference conditional and marginalized densities of equation (B-2) produce that of equation (B-6). This is achieved when

$$2\pi \left|\mathbf{P}_{x/z}\right|^{\frac{1}{2}} \left[2\pi\right]^{N_M} \left|\mathbf{P}_z\right|^{\frac{1}{2}} = \left[2\pi\sigma_p^2\right]^{N_M} 2\pi\sigma_{ref}^2 . \tag{B-20}$$

From equation (B-8), the determinant of the reference posterior covariance matrix becomes

$$\left|\mathbf{P}_{x/z}\right| = \left|\frac{\sigma_p^2}{N_M + \rho_p^2}\mathbf{I}_2\right| = \left(\frac{\sigma_p^2}{N_M + \rho_p^2}\right)^2 . \tag{B-21}$$

The marginal covariance matrix $\mathbf{P}_z$ of equation (B-13) is decoupled in the x and y Cartesian coordinates. Hence, if $\mathbf{P}_z$ is rearranged into block diagonal components corresponding to the two dimensions, then

$$\left|\mathbf{P}_z\right| = \begin{vmatrix} \mathbf{P}_{z_x} & \mathbf{0} \\ \mathbf{0} & \mathbf{P}_{z_y} \end{vmatrix} = \left|\mathbf{P}_{z_x}\right| \left|\mathbf{P}_{z_y}\right| . \tag{B-22}$$

Each coordinate covariance matrix takes the form of a symmetric compound matrix of the form

$$\mathbf{P}_{z_x} = \mathbf{P}_{z_y} = \sigma_p^2 \mathbf{I}_{N_M} + \mathbf{w}\mathbf{w}^T , \tag{B-23}$$

where $\mathbf{w} = \left[\sigma_{ref}, \sigma_{ref}, \ldots, \sigma_{ref}\right]^T$ is of size (N_M x 1). Hence, as in reference 15,

$$\begin{aligned} \left|\mathbf{P}_{z_x}\right| = \left|\mathbf{P}_{z_y}\right| &= \left|\sigma_p^2 \mathbf{I}_{N_M}\right| \cdot \left(1 + \mathbf{w}^T \left[\sigma_p^2 \mathbf{I}_{N_M}\right]^{-1} \mathbf{w}\right), \\ &= \sigma_p^{2N_M} \left(1 + \frac{N_M \sigma_{ref}^2}{\sigma_p^2}\right) = \sigma_p^{2N_M} \sigma_{ref}^2 \left(\frac{\rho_p^2 + N_M}{\sigma_p^2}\right). \end{aligned} \tag{B-24}$$

Substituting equations (B-21), (B-22), and (B-24) into equation (B-20) verifies the equality. Thus, the marginal density for object placement takes the form

$$f(\mathbf{x}_1, \ldots, \mathbf{x}_{N_M}) = \frac{1}{\left[2\pi\right]^{N_M}} \left(\frac{\sigma_p^{2-2N_M}}{\sigma_p^2 + N_M \sigma_{ref}^2}\right) \exp\left(-\frac{1}{2}\left[\mathbf{X} - \hat{\mathbf{X}}\right]^T \mathbf{P}_z^{-1} \left[\mathbf{X} - \hat{\mathbf{X}}\right]\right). \tag{B-25}$$

Rewriting the exponential in equation (B-25) with the form of $\mathbf{P}_z^{-1}$ from equation (B-12) leads to the following final form for the joint density:

$$f(\mathbf{x}_1,\ldots,\mathbf{x}_{N_M}) = \frac{1}{\left[2\pi\sigma_P^2\right]^{N_M}}\left(\frac{\rho_p^2}{N_M+\rho_p^2}\right)\exp\left\{-\frac{1}{2\sigma_P^2}\left(\sum_{j=1}^{N_M}(x_j-\hat{x}_j)^2+(y_j-\hat{y}_j)^2\right)\right\}$$
$$\times\exp\left\{-\frac{1}{2\sigma_P^2}\left(\frac{1}{N_M+\rho_P^2}\right)\left[\left(\sum_{j=1}^{N_M}x_j-\hat{x}_j\right)^2+\left(\sum_{j=1}^{N_M}y_j-\hat{y}_j\right)^2\right]\right\}. \quad \text{(B-26)}$$

APPENDIX C
GOAL-ORIENTED CURVILINEAR MOTION

This appendix describes the goal-oriented curvilinear motion (GOCM) model that is integrated as an external process within the search evaluation capability. The essence of GOCM kinematic modeling is as follows. All GOCM vehicular motion is modeled as being achieved under the condition of constant angular and radial acceleration. That is, let $\dot{C}$ and $\dot{S}$ denote constant change of course and speed rates, where C and S represent the vehicle course and speed, respectively, as functions of time. Then, for an initial time t_0 and arbitrary time t, $C(t) = C(t_0) + (t - t_0)\cdot\dot{C}$ and $S(t) = S(t_0) + (t - t_0)\cdot\dot{S}$. Using $\mathbf{x}(t) = [x(t) \quad y(t) \quad \dot{x}(t) \quad \dot{y}(t)]^T$ to denote a Cartesian coordinate representation of platform position and velocity, then $C(t) = \tan^{-1}(\dot{x}(t)/\dot{y}(t))$ and $S(t) = \sqrt{\dot{x}(t)^2 + \dot{y}(t)^2}$. To achieve constant velocity, course and speed rates are set to zero. This condition is indicative of a goal state satisfaction. More generally, the desired course and speed, C_{Goal} and S_{Goal}, will deviate from current values and induce a maneuvering trajectory. Consider ΔT as a search evaluation update interval. Let ΔT_1 denote the time necessary to achieve the first goal, regardless of which goal parameter it corresponds to. With maneuver times defined as

$$\Delta T_C = \text{Min}\left(\frac{|C_{Goal} - C(t_0)|}{\dot{C}}, \Delta T\right), \quad \Delta T_S = \text{Min}\left(\frac{|S_{Goal} - S(t_0)|}{\dot{S}}, \Delta T\right), \tag{C-1}$$

and with $\Delta T_1 = \text{Min}(\Delta T_C, \Delta T_S)$, the GOCM equations of state can be summarized as

$$\mathbf{x}(t) = \Phi(t_0, t)\,\mathbf{x}(t_0), \qquad \Phi(t_0, t) = \begin{bmatrix} 1 & 0 & A\cdot\Delta T & B\cdot\Delta T \\ 0 & 1 & -B\cdot\Delta T & A\cdot\Delta T \\ 0 & 0 & Dc & Ds \\ 0 & 0 & -Ds & Dc \end{bmatrix}, \tag{C-2}$$

where $Dc = (1 + \gamma\Delta T_S)\cos(\dot{C}\Delta T_C)$, $Ds = (1 + \gamma\Delta T_S)\sin(\dot{C}\Delta T_C)$, $\gamma = \dot{S}/S(t_0)$, $\delta = (1 + \gamma\Delta T_S)\cdot(\Delta T - \Delta T_C) - \gamma\cdot(\Delta T_S - \Delta T_1)^2/2$, and

$$\begin{aligned} A\cdot\Delta T &= (1 + \gamma\Delta T_1)\frac{\sin(\dot{C}\Delta T_C)}{\dot{C}} - \gamma\left[\frac{1 - \cos(\dot{C}\Delta T_1)}{\dot{C}^2}\right] + \delta\cos(\dot{C}\Delta T_C), \\ B\cdot\Delta T &= \frac{1 - (1 + \gamma\Delta T_1)\cos(\dot{C}\Delta T_C)}{\dot{C}} + \gamma\left[\frac{\sin(\dot{C}\Delta T_1)}{\dot{C}^2}\right] + \delta\sin(\dot{C}\Delta T_C). \end{aligned} \tag{C-3}$$

The GOCM model will produce search trajectories that exhibit a high degree of regularity. In particular, the sensor coverage methodology discussed in section 3 is applicable if the update interval ΔT is selected to constrain course and speed changes to nominal values where trajectory segments are approximately linear. Platform turn rates can be set to achieve specific search

patterns such as a "mow the lawn" path plan. Specifically, at the completion of a search leg, maintaining the speed S and setting C_{Goal} to C(t) + 180° and $\dot{C} = S/R_D$ will produce adjacent swaths of width $2R_D$. In addition, the area covered by the search swath from such a trajectory is identical to that obtained had a straight-line path been executed. To show this, observe that the area covered by a sensor of detection radius R_D during a turn of θ radians following a trajectory with radius of curvature of R_C, $R_C \geq R_D$ is

$$A_T = \theta/2 \cdot \left((R_C + R_D)^2 - (R_C - R_D)^2\right) = \theta \cdot 2R_C R_D . \tag{C-4}$$

A straight-line trajectory of swath width $2R_D$ will cover an area of

$$A_S = 2R_D \cdot S\Delta T_C . \tag{C-5}$$

With $R_C = R_D$ and $\Delta T_C = \theta/\dot{C} = \theta R_D/S$,

$$A_T = 2\theta R_D^2 = 2R_D \cdot S\Delta T_C . \tag{C-6}$$

With speed S constant, the constraint $\dot{C} = S/R_D$ yields a constant area coverage per unit time for non-overlapping search trajectories regardless of how often directed turns are made. As the probability assessments of section 2 are measures on sets relatable to area coverage, this result is useful for validating the calculated search performance against theoretical predictions using constant velocity search paths. Search path length $L_T = S \cdot \Delta T_C = \theta R_D$ is also identical for the straight and curvilinear trajectories under these conditions.

INITIAL DISTRIBUTION LIST

Addressee	No. of Copies
Office of Naval Research (M. Traweek, M. Wardlaw, T. Swean)	3
Naval Sea Systems Command (PMS-395—J. Stack, M. Cramer, G. Saroch)	3
Naval Surface Warfare Center, Panama City (P. Adair, J. Hyland, C. Smith, K. Stence)	4
Defense Technical Information Center	2